



# Unriddle the complex associations among urban green cover, built-up index, and surface temperature using geospatial approach: a micro-level study of Kolkata Municipal Corporation for sustainable city

Md Babor Ali<sup>1</sup> · Saleha Jamal<sup>1</sup> · Manal Ahmad<sup>1</sup> · Mohd Saqib<sup>1</sup>

Received: 2 December 2023 / Accepted: 29 January 2024 / Published online: 16 February 2024  
© The Author(s), under exclusive licence to Springer-Verlag GmbH Austria, part of Springer Nature 2024

## Abstract

The research article delves into the background of urban land use and land cover (LULC) change, specifically focusing on built-up expansion, and underscores its significant implications on land surface temperature (LST) and the urban heat island (UHI) phenomenon. This research aims to unravel the intricate associations among urban green cover, built-up index, and surface temperature, specifically within the spatial confines of the Kolkata Municipal Corporation. The primary objective is to comprehensively understand how the conversion of green spaces into built-up areas influences land surface temperature and, consequently, the urban heat island effect. Employing a geospatial approach, the study utilizes normalized differential vegetation index (NDVI), normalized differential built-up index (NDBI), and land surface temperature (LST) data extracted from Landsat imagery spanning four temporal points (1990, 2000, 2010, and 2020). The borough-level analysis offers a micro-level perspective within the limited urban space of Kolkata Municipal Corporation. Correlation analyses and scatter diagrams are employed as tools to scrutinize the complex relationships between these variables, providing a robust methodology for the investigation. The research underscores the significant impact of urbanization on the study area, revealing a consistent trend of converting green spaces into built-up areas over the studied decades. This transformation has led to a reduction in green coverage and a concurrent increase in surface temperatures. The study reveals compelling correlations and patterns through NDVI, NDBI, and LST analyses, emphasizing the urgency for serious attention from urban planners, environmentalists, and ecologists. The findings highlight the pressing need for the development of appropriate policy frameworks to ensure the future sustainability and health of cities.

## 1 Introduction

In the past three decades, rapid expansion in urban areas has gone through, and over 53% of the world's population now lives in urban areas (United Nations Department of Economic and Social Affairs (UNDESA), 2012; Moghadam and

Helbich 2013). This percentage is anticipated to rise to more than 60% of the overall population by 2030 (Demographia 2017) and more than 72% by 2050 (United Nations 2012). Due to rapid urbanization in terms of population growth and geographic expansion, particularly in India, there is a steady loss of natural resources especially urban green spaces (The World Resources Institute 1996; Xian et al. 2005; Mushore et al. 2017; Sannigrahi et al. 2018; Jamal et al. 2022a, b). Cities around the world, including in India, are experiencing a continuous reduction of urban green spaces as a result of growing urbanization in terms of both population and spatial growth (Chadchan and Shankar 2012). The World Resources Institute examined and documented this extensively in 1996 (Xian et al. 2005). In addition, agricultural land located primarily on the outskirts of urban areas is converted into built-up areas (Pandey and Seto 2015). This alteration in land use and land cover has a detrimental effect on agricultural and

---

✉ Saleha Jamal  
salehajm@gmail.com

Md Babor Ali  
baboraliamu@gmail.com

Manal Ahmad  
manalah1807@gmail.com

Mohd Saqib  
saqibalig98@gmail.com

<sup>1</sup> Aligarh Muslim University, Aligarh, Uttar Pradesh 202001, India

forest lands, resulting in the expansion of barren regions and the increase of impermeable surfaces (Kumar et al. 2012; Sarif et al. 2022). As a result, the decrease in greenery and the expansion of urban development are anticipated to increase the land surface temperature (Shahfahad et al. 2021; Mohammad and Goswami 2022; Naikoo et al. 2022; García et al. 2023). The presence of green spaces is crucial in urban areas as it fosters a healthier city environment, encourages well-being, and maintains the visual and ecological attractiveness of the area (Lillesand et al. 2015). All aspects and processes on earth's surface are closely interconnected, leading to substantial influences on the nearby surroundings. These interdependencies are so profound that a change in one factor can set off indirect consequences for others (Weng 2001). The attributes of the earth's surface, encompassing its physical, chemical, and biological traits, are influenced by factors such as the energy balance, atmospheric conditions, thermal characteristics of the surface, and the properties of the surface materials. These elements collectively impact the land surface temperature (Becker and Li 1990).

India has witnessed remarkable urban expansion over recent decades, with the number of cities boasting a population of one million or more increasing from 23 in 1991 to 53 in 2011. Additionally, the urban population surged from 109 million in 1971 to 377 million in 2011, accounting for 19.9% and 31.6% of the total population, respectively (Census 2011). This trend of urbanization has led to a significant reduction in urban green areas, as documented in various studies (Chudnovsky et al. 2004; Yogesh et al. 2009; Mushore et al. 2017; Sannigrahi et al. 2018; Jamal et al. 2022a, b; Jamal et al. 2023). Studies have shown a connection between land surface temperature, developed urban areas, the presence of green spaces, and the phenomenon known as the urban heat island (UHI) effect. This relationship has been established in research conducted by various scholars (Badarinath et al. 2005; Mallick et al. 2008; Shahfahad et al. 2023). The rise in land surface temperature results in the formation of urban heat islands and shifts in the urban climate (Rinner and Hussain 2011; Feng et al. 2014). Consequently, this brings about noteworthy adverse effects on crucial environmental parameters, including elevated levels of atmospheric greenhouse gases (Loehle and Scafetta 2011; Hartmann et al. 2013), disruptions in energy and water equilibrium (Sertel et al. 2011; Nayak and Mandal 2012; Ward et al. 2014), occurrences of heatwaves and air quality concerns (Chudnovsky et al. 2004), diminished carbon sequestration, reduced evapotranspiration and cooling effects (Oliveira et al. 2011a, b), and a decline in biodiversity (McKinney 2002; Karuppanan et al. 2014). The rise in surface air temperature, coupled with the changing landscape of urban green spaces, has notably adverse impacts on ecosystem sustainability (Hao et al. 2016). When evaluating the well-being of the environment, it is of utmost importance

to consider the existence of urban green spaces as a fundamental element of the urban ecosystem (Carrus et al. 2015; Ajmal et al. 2022). These green spaces exert a significant impact on the advancement of sustainable urban development and the improvement of human health and overall quality of life. Numerous research studies have demonstrated that urban green spaces offer a wide array of ecological advantages (Gairola and Noresah 2010; Escobedo et al. 2011). These range from the mitigation of climate change and the reduction of pollution to the purification of air and water, the regulation of microclimates, the support of wildlife, and the conservation of biodiversity, as well as the provision of protection against flooding and other environmental risks (Konijnendijk et al. 2013). Moreover, a multitude of supplementary research endeavors have substantiated the notable impact of green spaces in urban regions on the encompassing natural ecosystem and the overall urban milieu (Nowak et al. 2010; Wolch et al. 2014a; Zhang et al. 2014).

The appraisal and scrutiny of modifications in the environment, including the evaluation of land surface temperature and the manifestation of the urban heat island phenomenon, are typically executed by means of remote sensing data acquired from satellites (Ma et al. 2010; Deng and Wu 2012; Xu et al. 2013). This facilitates the identification of developing patterns during specific intervals of time (Mass 1999; Li and Yang 2004; Salman 2004; Yuan et al. 2005; Mallick et al. 2013; Mathew et al. 2016). In addition, the computation and evaluation of indicators such as land surface temperature (LST), normalized difference vegetation index (NDVI), and normalized difference built-up index (NDBI) to monitor changes in environmental aspects of urban ecosystems have heavily relied on the utilization of remote sensing and Geographic Information System (GIS) techniques (Asgarian et al. 2015; Guo et al. 2015; Mohan and Kandya 2015; Rotem-Mindali et al. 2015). For example, numerous research studies have established a significant association between LST and the extent of constructed areas and vegetation coverage (Bindi et al. 2009; Buyadi et al. 2013; Feng et al. 2014; Asgarian et al. 2015; Shahfahad et al. 2021; Jamal et al. 2023). These variables are employed to indicate the impact of urbanization on alterations in LST, constructed areas, vegetation cover, and ultimately the emergence of the urban heat island (UHI) phenomenon (Kaufmann et al. 2003; Weng et al. 2004; Kumar et al. 2012). Furthermore, multiple investigations have delved into the causal connections between constructed areas, vegetation coverage, and LST (Badarinath et al. 2005; Guangyong You et al. 2013).

In the present contextual framework, the usage of multi-temporal Landsat data proves to be highly advantageous when assessing alterations in surface temperature over a span of 10 years (Weng 2001; Chen et al. 2002; Buyadi et al. 2013). The utilization of the thermal band in Landsat imagery is notably efficient in obtaining surface temperature

data for any specified region, a fact that is substantiated by various sources. Regions characterized by elevated LST are frequently associated with tall residential and industrial structures but limited vegetation. NDVI and NDBI have emerged as more dependable tools for quantitatively examining LST fluctuations across different time intervals in urbanized areas (Li and Yang 2004; Chen et al. 2006; Yuan and Bauer 2007). The surface temperatures in built-up, commercial, and industrial zones consistently surpass those in surrounding regions with more extensive green spaces. Furthermore, an expansion in green areas demonstrates a cooling effect on both the surrounding urban built-up regions and within lush zones (Hang and Rahman 2018a). Consequently, this investigation aims to scrutinize the interconnectedness between built-up and green coverage and its impact on surface temperature. To fulfill this objective, authors perform an analysis at the borough and sub-division level of NDVI, NDBI, and LST within the very small urban area encompassed by the Kolkata Municipal Corporation from the mega city Kolkata.

## 2 Literature review

Wu et al. (2019) investigate the effects of land conversion, urbanization, and infrastructure development on the quantity, quality, and accessibility of green spaces, stressing the necessity of integrated land use planning, green infrastructure design, and ecosystem-based management to safeguard and improve urban green spaces. In their study, Zhou and Wang (2011) investigate the impact of urban growth, land development, and infrastructure expansion on green space availability, accessibility, and functionality, highlighting the crucial role of sustainable urban planning and green infrastructure strategies in alleviating the effects of urbanization. In their study, Li et al. (2017) investigate the effects of land conversion, urbanization, and infrastructure development on the quantity, quality, and accessibility of green spaces, while discussing both challenges and opportunities for sustainable land use planning, green infrastructure design, and the conservation of urban biodiversity. In their research, Pauleit et al. (2005) analyze the impacts of land conversion, fragmentation, and degradation on green spaces' ecological functions, biodiversity, and microclimate, underscoring the significance of integrating long-term sustainability and resilience into urban planning and land use management practices.

Wolch et al. (2014a) explored the connections between urban green spaces, public health, and environmental justice, underscoring the positive impact of green areas in mitigating heat-related health issues in urban environments while advocating for equitable distribution of these spaces for environmental justice. Oliveira et al. (2011a, b) focused on assessing

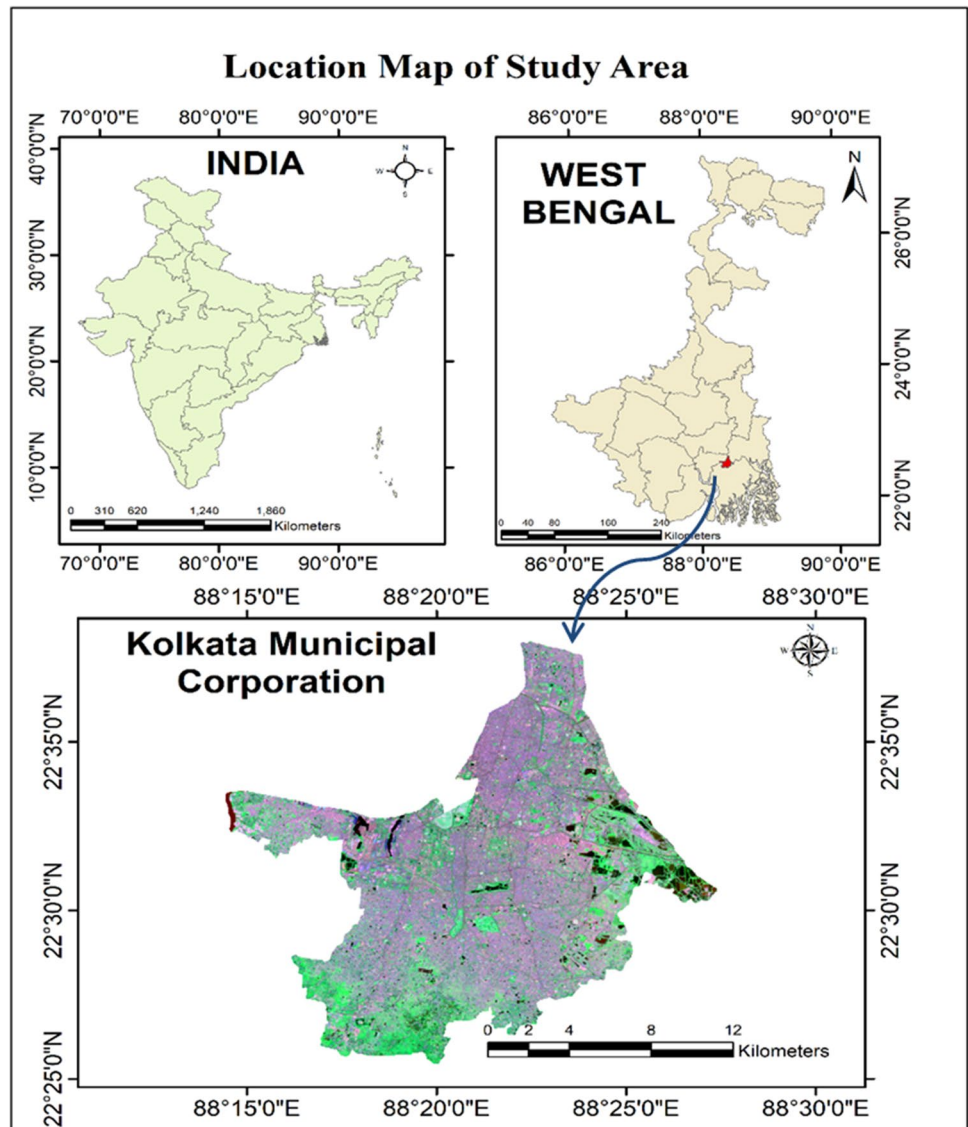
the cooling effect of green spaces in Madrid, Spain, revealing that these areas significantly reduce land surface temperatures, especially during heatwaves, highlighting the importance of green space configuration and spatial distribution to maximize cooling potential. Rosenzweig et al. (2006) summarized research findings on the role of urban green spaces in mitigating urbanization's adverse effects, particularly the urban heat island phenomenon. Zhang et al. (2020)'s systematic study showed that urban green spaces contribute to temperature reduction through shading, evaporative cooling, and moisture release, significantly lowering surface temperatures in urban environments. Jim and Chen (2008) assessed urban trees' air pollutant removal service in Guangzhou, China, finding that they effectively mitigate the heat island effect by enhancing air quality and contributing to a more favorable microclimate with lower surface temperatures. Alavipanah et al. (2015) conducted a meta-analysis synthesizing multiple studies to evaluate vegetation's role in mitigating urban land surface temperatures, quantifying cooling effects, and providing insights into optimal vegetation characteristics and configurations for temperature control. Wu et al. (2021) analyzed empirical evidence concerning the relationship between green spaces and land surface temperature reduction in urban areas, discussing the cooling effects of various green space types like urban parks, gardens, and green corridors, and highlighting challenges and opportunities in integrating green spaces into urban planning and design.

## 3 Materials and methods

### 3.1 Study area

Kolkata Municipal Corporation (KMC) is situated in the eastern part of India, serving as the administrative and urban hub of West Bengal and it is one of the four municipal corporations consisting of the entire mega city Kolkata. It encompasses an area of approximately 206 km<sup>2</sup> along the banks of the Hooghly River, a distributary of the Ganges. KMC is the local governing body of the city of Kolkata, India, which is responsible for administering and providing public services such as sanitation, water supply, waste management, and infrastructure development to the citizens of Kolkata. The KMC was established in 1876 and is one of the oldest municipal corporations in the country and is divided into 16 boroughs (Fig. 1). The population density of the KMC remains very high at 21,739 individuals per square kilometer. Kolkata is experiencing rapid urbanization and population growth, which poses significant challenges to the KMC in managing and developing the city's infrastructure and services. The city's geographical conditions have played a significant role in shaping its urban landscape. Kolkata's topography is relatively flat, with some small undulations

**Fig. 1** Locational map of the study area



and raised areas. The soil composition primarily consists of alluvial deposits, making it fertile for agriculture in the surrounding regions. Kolkata experiences a tropical wet-and-dry climate characterized by distinct monsoon and dry seasons. The city's proximity to the Bay of Bengal influences its weather patterns, leading to high humidity levels, particularly during the summer months. The annual average temperature hovers around 26 °C, with peak summer temperatures often exceeding 30 °C. Overall, Kolkata's geographical conditions have influenced its development and continue to shape urban planning efforts, especially in the context of climate resilience and sustainable development. Efforts to manage natural resources, especially green spaces, and address issues of microclimate are paramount

in ensuring the city's continued growth and well-being of its inhabitants.

### 3.2 Database

Satellite data and GIS techniques are considered highly reliable and valuable tools for monitoring urban green spaces, built-up areas, and microclimatic patterns due to their comprehensive and repetitive coverage (Smith et al., 1998). In this current investigation, multi-temporal Landsat satellite data was employed. Landsat-5 TM data from 1990, 2000, and 2010 were utilized, while Landsat-8 OLI data was employed for the year 2020. The satellite data was sourced from the USGS Earth Explorer web portal (<https://earth>

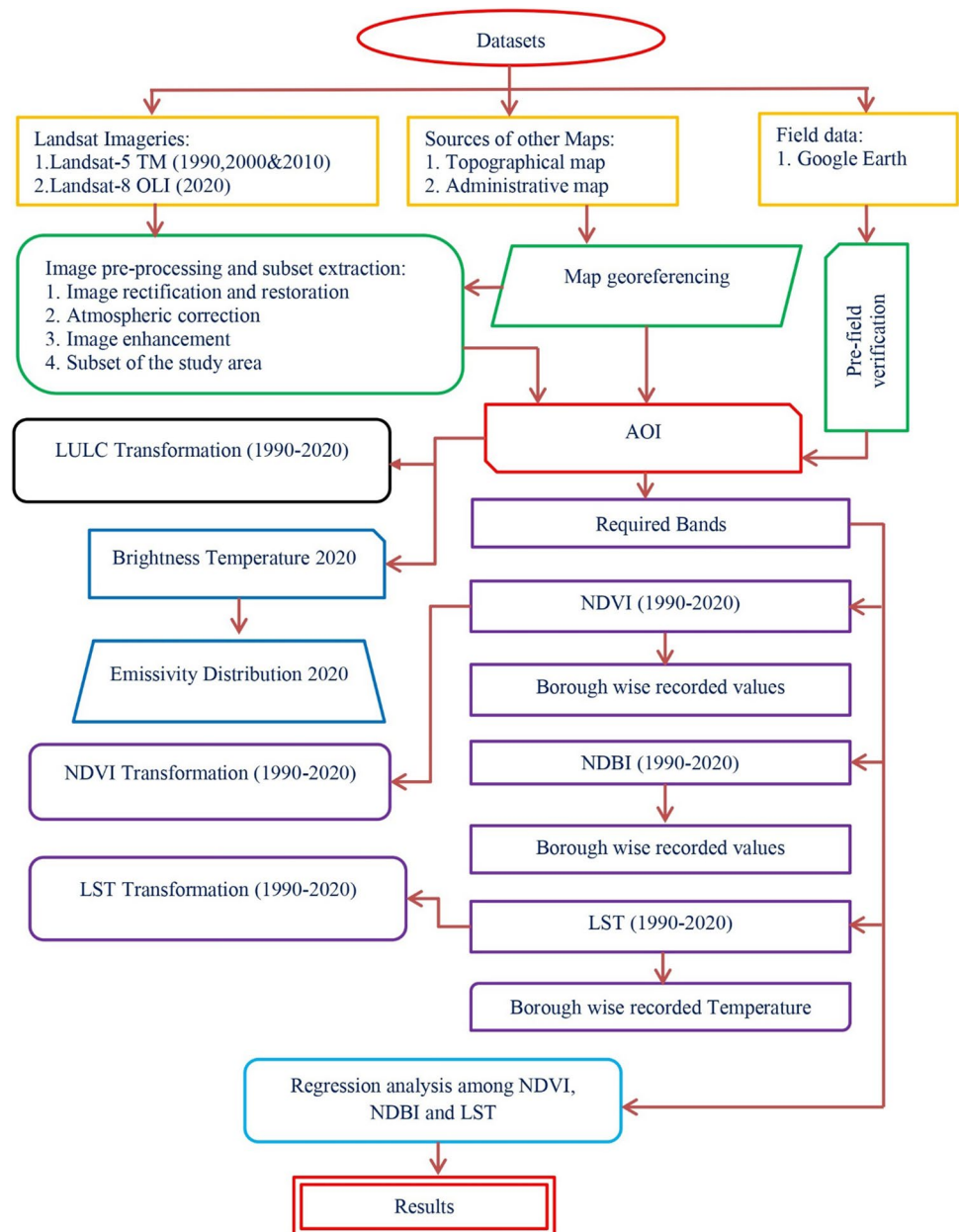
explorer.usgs.gov) with a preference for cloud and haze-free imagery. These images underwent initial georeferencing and rectification during preprocessing. The UTM (Universal Transverse Mercator) zone 45 N projection, based on the WGS 84 datum, was applied to these images. Image registration was performed using the nearest neighbor resampling method, involving 25 ground control points (GCPs) to ensure maximum overlay accuracy. The spatial resolution for all images is 30 m, with a consistent path and row of 138 and 44 respectively. This uniform spatial resolution enhances the precision of GIS-based maps for various features. Additionally, Google Earth Pro was employed to collect GCP samples, facilitating associations between green spaces, built-up

areas, and surface temperature. Topographical and administrative maps were also consulted for this study.

### 3.3 Methods

The processing of the data was carried out by researchers using Arc GIS 10.5 software to stack and extract a particular area of interest (AOI) utilizing the latest boundary map of Kolkata Municipal Corporation. The normalized differential built-up index (NDBI), normalized differential vegetation index (NDVI), and land surface temperature (LST) were calculated for the years 1990, 2000, 2010, and 2020. Further, a cross-sectional surface temperature profile

Fig. 2 Methodological flow-chart



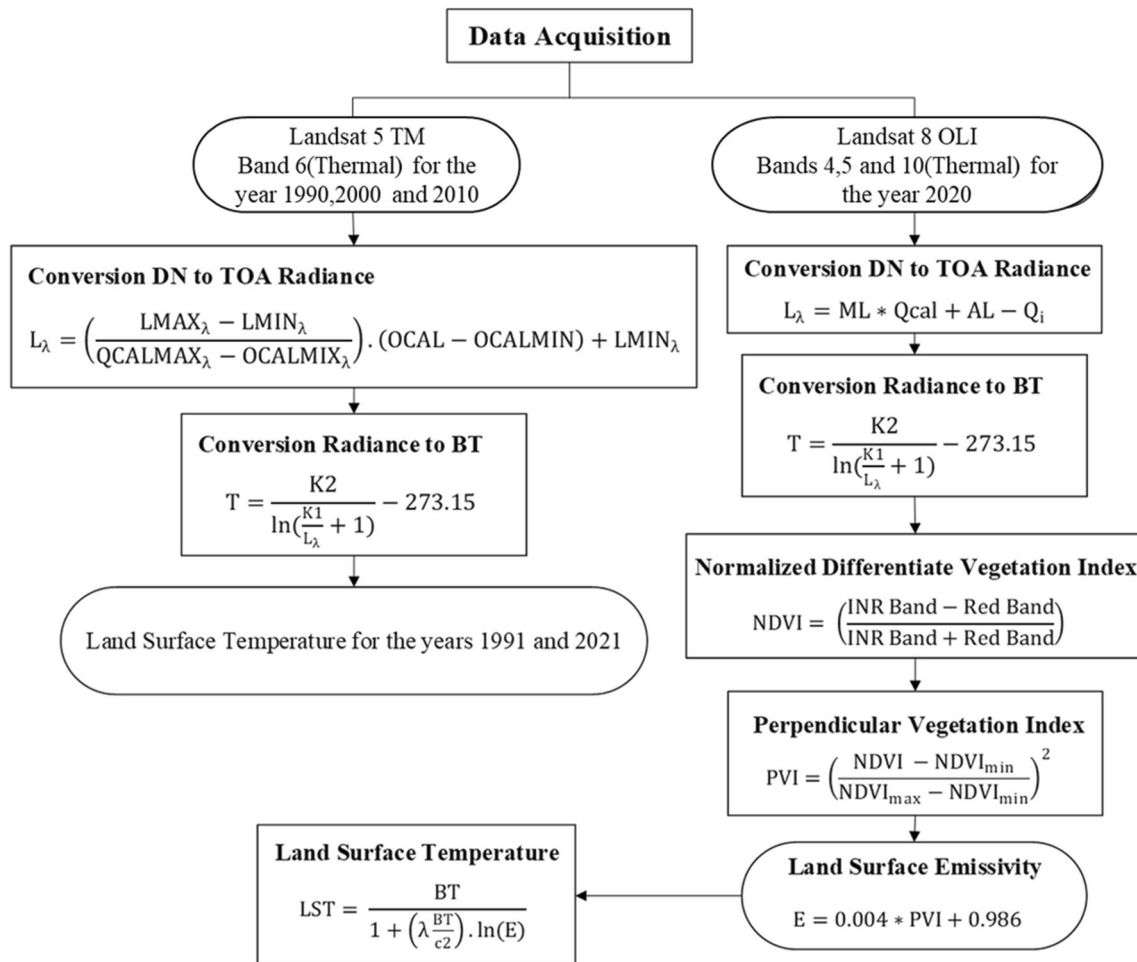


**Fig. 3** Flowchart of land surface temperature calculation

was constructed to make a comparative analysis of same places observed temperature over the last three decades with 10 years of time interval. Additionally, borough-wise analysis was performed by extracting NDBI, NDVI, and LST using clip tools in ArcGIS 10.5 software. To scrutinize the association between built-up and vegetation cover with land surface temperature (LST), a statistical analysis through the usage of the Social Science Statistical Package (SPSS) software is conducted. Additionally, a scatter plot is devised to evaluate the correlation among the variables, as depicted in Figs. 13 and 14. The details of methodology are given in the below flowcharts (Fig. 2 and Fig. 3).

### 3.4 Calculation of normalized difference vegetation index

The computation of the normalized difference vegetation index (NDVI) is attained through Eq. 1, which was originally presented by Gao (1996). The Landsat data's red and infrared bands are employed in this

computation. The rationale behind using the near-infrared (NIR) and red bands ratio is due to the fact that chlorophyll exhibits the highest absorption in these two bands of the electromagnetic spectrum, as stated by Bindi et al. (2009). The NDVI formula is expressed as follows:

$$NDVI = \frac{\text{Near Infrared(NIR)} - \text{Red}}{\text{Near Infrared(NIR)} + \text{Red}} \quad (1)$$

### 3.5 Calculation of normalized difference built-up index

The computation of the normalized difference built-up index (NDBI) is executed by utilizing the short wave infrared (SWIR) and near-infrared (NIR) bands of Landsat data. Equation 2, presented by Zha et al. (2003), is utilized for this purpose. The NDBI formula is expressed as follows:

$$\text{NDBI} = \frac{\text{SWIR} - \text{NIR}(\text{NearInfrared})}{\text{SWIR} + \text{NIR}(\text{NearInfrared})} \quad (2)$$

### 3.6 Calculation of LST from thermal band of Landsat 5 TM

To obtain the land surface temperature (LST) for Landsat 5 TM, a series of steps are undertaken (Fig. 3). Firstly, the digital number of the image is converted into spectral radiance by employing the rigorous Eq. 3:

$$L(\lambda) = (2hc^2/\lambda^5)/(\exp(hc/\lambda kT) - 1) \quad (3)$$

In this equation,  $L(\lambda)$  denotes the spectral radiance at wavelength  $\lambda$ ,  $h$  refers to Planck's constant,  $c$  represents the speed of light,  $k$  is Boltzmann's constant,  $T$  signifies the temperature of the object, and  $\lambda$  refers to the wavelength. Subsequently, the spectral radiance is transformed into at-satellite brightness temperature in Kelvin ( $T(K)$ ) by utilizing Eq. 4:

$$T(K) = (c^2/(2 * k * v^2)) * \ln((2 * h * v^3)/(c^2 * (\exp((h * v)/(k * T_b)) - 1))) \quad (4)$$

Here,  $T(K)$  represents the brightness temperature in Kelvin,  $c$  denotes the speed of light in meters per second (approximately  $3 \times 10^8$  m/s),  $k$  is the Boltzmann constant in joules per Kelvin (approximately  $1.38 \times 10^{-23}$  J/K),  $v$  is the frequency of the radiation in hertz,  $h$  signifies the Planck constant in joule-seconds (approximately  $6.63 \times 10^{-34}$  J-s), and  $T_b$  denotes the brightness temperature in Kelvin. Furthermore, the conversion constants  $K1$  and  $K2$  are pre-launch calibration constants ( $K1 = 1260.56$  and  $K2 = 607.66$  mWcm-2sr-1), and  $b$  represents an effective spectral range ( $b = 1.239 \mu\text{m}$ ) when the response of sensor is above 50%.

### 3.7 Calculation of LST from thermal band of Landsat 8 OLI/TIRS

For Landsat 8 OLI/TIRS, the retrieval of LST involves a different procedure (Fig. 3). Initially, the OLI and TIRS band data are converted to spectral radiance utilizing Eq. 5:

$$L\lambda = (ML * Q_{cal}) + AL \quad (5)$$

Here,  $L\lambda$  denotes the temperature of the atmosphere's spectral radiance.  $ML$  represents the multiplicative rescaling factor specific to each band.  $AL$  represents the additive rescaling factor specific to each band.  $Q_{cal}$  represents the pixel values (DN) of the quantized and calibrated standard product. Afterward, the reflectance rescaling coefficients provided in the product metadata

file (MTL file) are used to transform the band data into reflectance, Eq. 6:

$$\rho\lambda' = M\rho * Q_{cal} + A\rho \quad (6)$$

Here, the reflectance for a particular band ( $\lambda$ ) is denoted as  $\rho\lambda'$ . The band-specific multiplicative rescaling factor is represented by  $M\rho$ , while the band-specific additive rescaling factor is denoted as  $A\rho$ . The quantized and calibrated standard product pixel values (DN) for that band are indicated by  $Q_{cal}$ .

### 3.8 Conversion of radiance into brightness temperature or LST

Finally, for TIRS band data, the spectral radiance is converted to brightness temperature using the thermal constants provided in the metadata file, Eq. 7:

$$\text{BT} = K2/(\ln(K1/L\lambda + 1) + \ln h) \quad (7)$$

Here,  $\text{BT}$  represents the at-satellite brightness temperature in Kelvin,  $K1$ ,  $K2$ , and  $L\lambda$  are the band-specific thermal conversion constants, and  $\ln h$  is the natural logarithm.

### 3.9 Conversion of LST data from Kelvin to degree Celsius

Lastly, Eq. 8 is employed by Jamal et al. (2023) to calculate the radiant temperature in Celsius, which is:

$$T(^{\circ}\text{C}) = \text{BT} - 273.15 \quad (8)$$

In this equation,  $T(^{\circ}\text{C})$  signifies the radiant temperature in Celsius, and  $\text{BT}$  denotes the at-satellite brightness temperature in Kelvin.

### 3.10 Calculating the proportion of vegetation

The determination of vegetation proportion, denoted as  $PV$ , is achieved through the utilization of a specific formula. This formula involves the calculation of radiance, satellite temperature, and the vegetation index. The formula, as outlined by Barsi et al. (2014), is expressed as follows:

$$PV = (5) \left[ \frac{(\text{NDVI} - \text{NDVI}_{\text{min}})}{(\text{NDVI}_{\text{max}} - \text{NDVI}_{\text{min}})} \right]^2 \quad (9)$$

where  $PV$  represents the proportion of vegetation,  $\text{NDVI}_{\text{min}}$  signifies the minimum value of NDVI, and  $\text{NDVI}_{\text{max}}$  represents the maximum value of NDVI.

### 3.11 Regression analysis

In this particular investigation, a correlation has been established among various variables. In order to illustrate this

correlation, a scatter plot was created with the inclusion of a linear regression line. The scatter plot was generated using MS Excel 2021 along with the linear regression Eq. (10),

$$Y_c = a + b \quad (10)$$

Here,  $Y_c$  denotes the estimated value,  $a$  represents the  $y$ -intercept, and  $b$  signifies the regression coefficient. The values of  $a$  and  $b$  are determined by the following formulas:

$$b = \frac{N \sum XY - \sum X \sum Y}{N \sum X^2 - (\sum x)^2}, a = \frac{\sum Y - b \sum x}{N}$$

## 4 Results and discussion

### 4.1 Transformation in vegetation index and association with thermal condition

Table 1 presents the highest and lowest normalized difference vegetation index (NDVI) recorded in different boroughs for the years 1990, 2000, 2010, and 2020. NDVI is a measure of the amount and health of vegetation in an area. For each borough, the table provides two values for each year, the highest NDVI value (indicating the most vegetation) and the lowest NDVI value (indicating the least vegetation). The data reveals a consistent decline in areas classified as dense and sparse vegetation from 1990 to 2020. In contrast, the areas classified as other land use and land cover have experienced a significant increase during the same period. This reduction in dense vegetation is considered one of the main

factors contributing to the rise in land surface temperature. Furthermore, the green spaces with sparse vegetation, characterized by an NDVI index, have also deteriorated over time. To further analyze the data, a ward-wise interpretation of the NDVI indices has been conducted. This would involve examining the changes in land use and land cover within each ward or administrative division. By analyzing the NDVI indices at a more localized level, it would be possible to identify specific areas or regions that have experienced significant changes in vegetation density and land use over time. This information can be valuable for understanding the impact of these changes on the local environment and for implementing targeted conservation and land management strategies.

For example, in borough 1, the highest NDVI value in 2020 was 0.467, while the lowest was  $-0.047$  (Fig. 4). This means that in 2020, the area of borough 1 with the most vegetation had an NDVI value of 0.467, while the area with the least vegetation had an NDVI value of  $-0.047$ . The table shows that the NDVI values can vary greatly within a borough and over time. For instance, in borough 7, the highest NDVI value increased from 0.705 in 1990 to 0.613 in 2010, but then decreased to 0.485 in 2020. Similarly, the lowest NDVI value in borough 7 decreased from  $-0.682$  in 1990 to  $-0.209$  in 2010, but then increased to  $-0.073$  in 2020. Boroughs with higher levels of urbanization may have lower NDVI values due to the presence of buildings, roads, and other infrastructure, which can limit the growth of vegetation. Conversely, boroughs with less urbanization may have higher NDVI values as they have more open spaces and green areas. Boroughs with higher NDVI values may have implemented conservation efforts, such as reforestation

**Table 1** Borough wise recorded highest and lowest NDVI for 2020, 2010, 2000, and 1990

Boroughs	2020		2010		2000		1990	
	Highest	Lowest	Highest	Lowest	Highest	Lowest	Highest	Lowest
1	0.467	$-0.047$	0.527	$-0.217$	0.417	$-0.170$	0.655	$-0.474$
2	0.416	0.012	0.437	$-0.086$	0.275	$-0.094$	0.443	$-0.476$
3	0.478	$-0.057$	0.562	$-0.189$	0.469	$-0.167$	0.588	$-0.333$
4	0.378	$-0.041$	0.419	$-0.137$	0.259	$-0.132$	0.519	$-0.278$
5	0.405	$-0.091$	0.476	$-0.200$	0.406	$-0.191$	0.518	$-0.561$
6	0.479	$-0.014$	0.449	$-0.107$	0.377	$-0.115$	0.553	$-0.446$
7	0.485	$-0.073$	0.613	$-0.209$	0.496	$-0.160$	0.705	$-0.682$
8	0.423	$-0.072$	0.505	$-0.179$	0.462	$-0.137$	0.645	$-0.690$
9	0.483	$-0.094$	0.541	$-0.375$	0.477	$-0.259$	0.741	$-0.534$
10	0.480	$-0.098$	0.556	$-0.106$	0.478	$-0.107$	0.652	$-0.563$
11	0.473	$-0.059$	0.533	$-0.156$	0.473	$-0.098$	0.687	$-0.436$
12	0.496	$-0.159$	0.600	$-0.265$	0.472	$-0.143$	0.685	$-0.836$
13	0.456	$-0.063$	0.575	$-0.163$	0.504	$-0.132$	0.667	$-0.540$
14	0.556	$-0.048$	0.565	$-0.163$	0.521	$-0.102$	0.641	$-0.632$
15	0.478	$-0.088$	0.603	$-0.375$	0.472	$-0.292$	0.766	$-0.340$
16	0.556	$-0.086$	0.583	$-0.149$	0.548	$-0.148$	0.695	$-0.333$



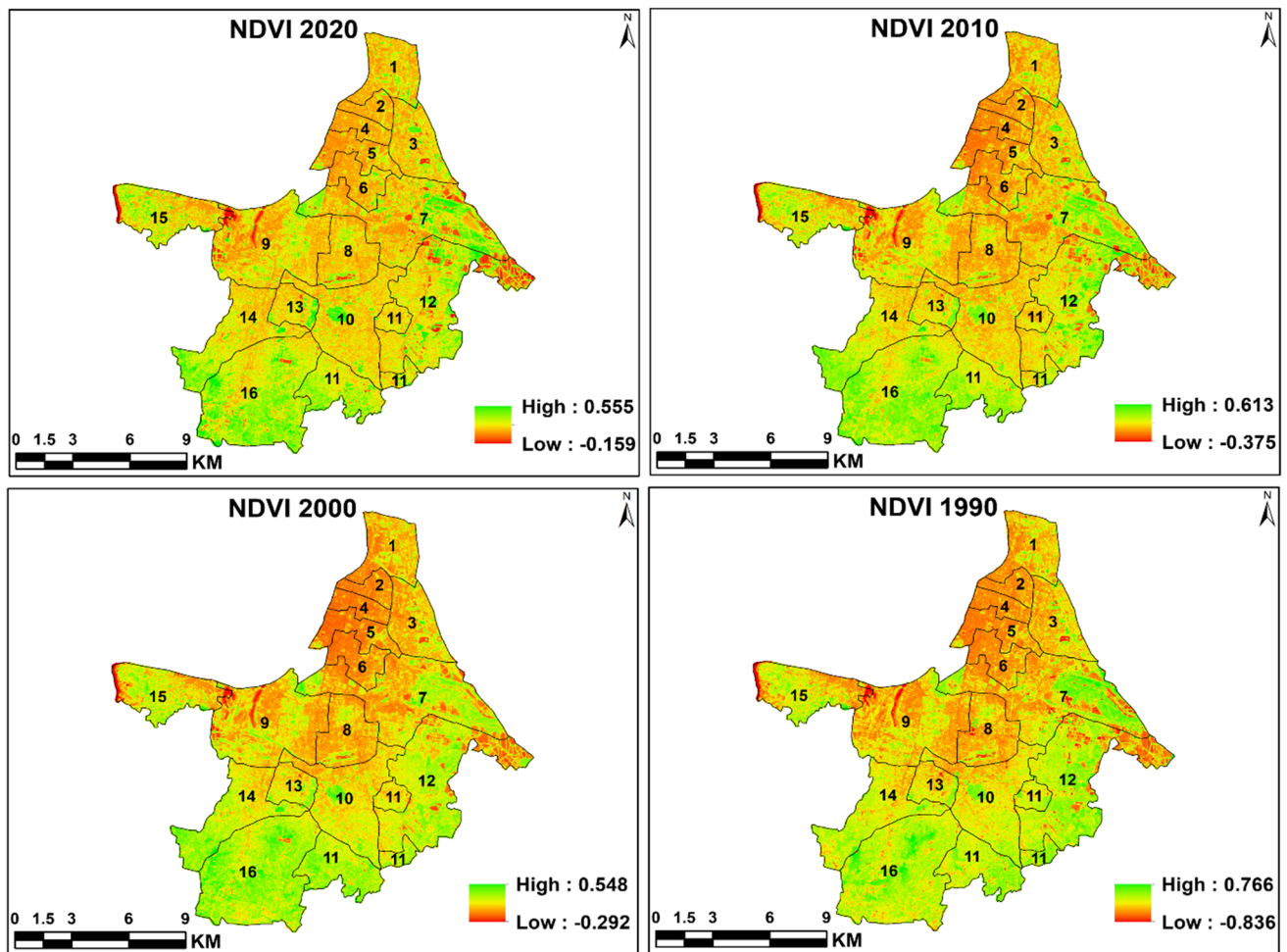


Fig. 4 Decadal maps of normalized difference vegetation index (1990–2020)

or afforestation programs, which have positively influenced vegetation growth. The transformation trend shown in Fig. 5 highlights that the major transformation has been taken place in boroughs 11, 12, and 16. As a result, a significant increase in temperature trend could be noticed in these years (1990–2020) with an equivalent decrease in green spaces. It can also be deduced that there has been a decline in NDVI within the urban core as time has progressed. It has been recorded in previous scholarly investigations that there exists a strong negative or inverse correlation between NDVI and LST, with ample coefficient of determinations (Fig. 13).

#### 4.2 Transformation in built-up index and association with thermal condition

The normalized difference built-up index (NDBI) is a measure used in remote sensing to identify built-up areas. Table 2 presents the highest and lowest normalized difference built-up index for each borough of the Kolkata Municipal Corporation for the years 2020, 2010, 2000, and 1990. For each

borough and year, two values are recorded, i.e., the highest and lowest. For example, in 2020, the highest built-up index in borough 1 was 0.139, while the lowest was  $-0.311$ . Similarly, in 1990, the highest built-up index in borough 1 was 0.603, while the lowest was  $-0.634$ . The table allows for comparison of urban development and changes in built-up areas across different boroughs and over time. Negative values indicate less built-up areas, while positive values indicate higher built-up areas. This data can be used to understand urban growth patterns, plan urban development, and manage urban spaces effectively. Several researchers have conducted research and discovered a significant connection between high temperatures and regions characterized by a dense population, intense industrialization, and a multitude of structures (Su et al. 2012; Lillesand et al. 2015; Shahfahad et al. 2021). To further explore the phenomenon known as the urban heat island effect, they employed the utilization of Landsat TM/ETM+ images, as well as the application of NDVI and NDBI indices. Their investigation yielded the result that impermeable surfaces are linked to elevated land

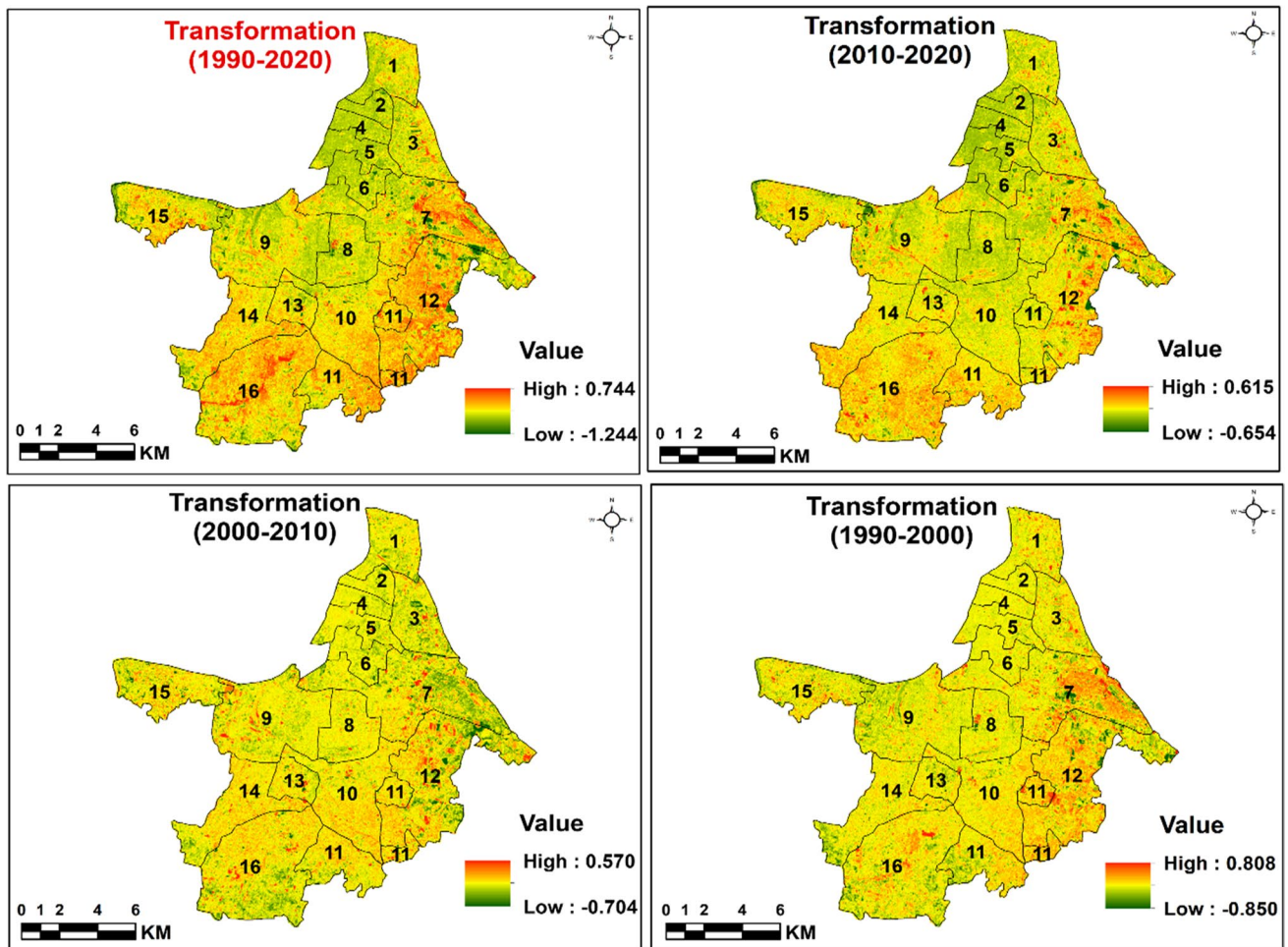
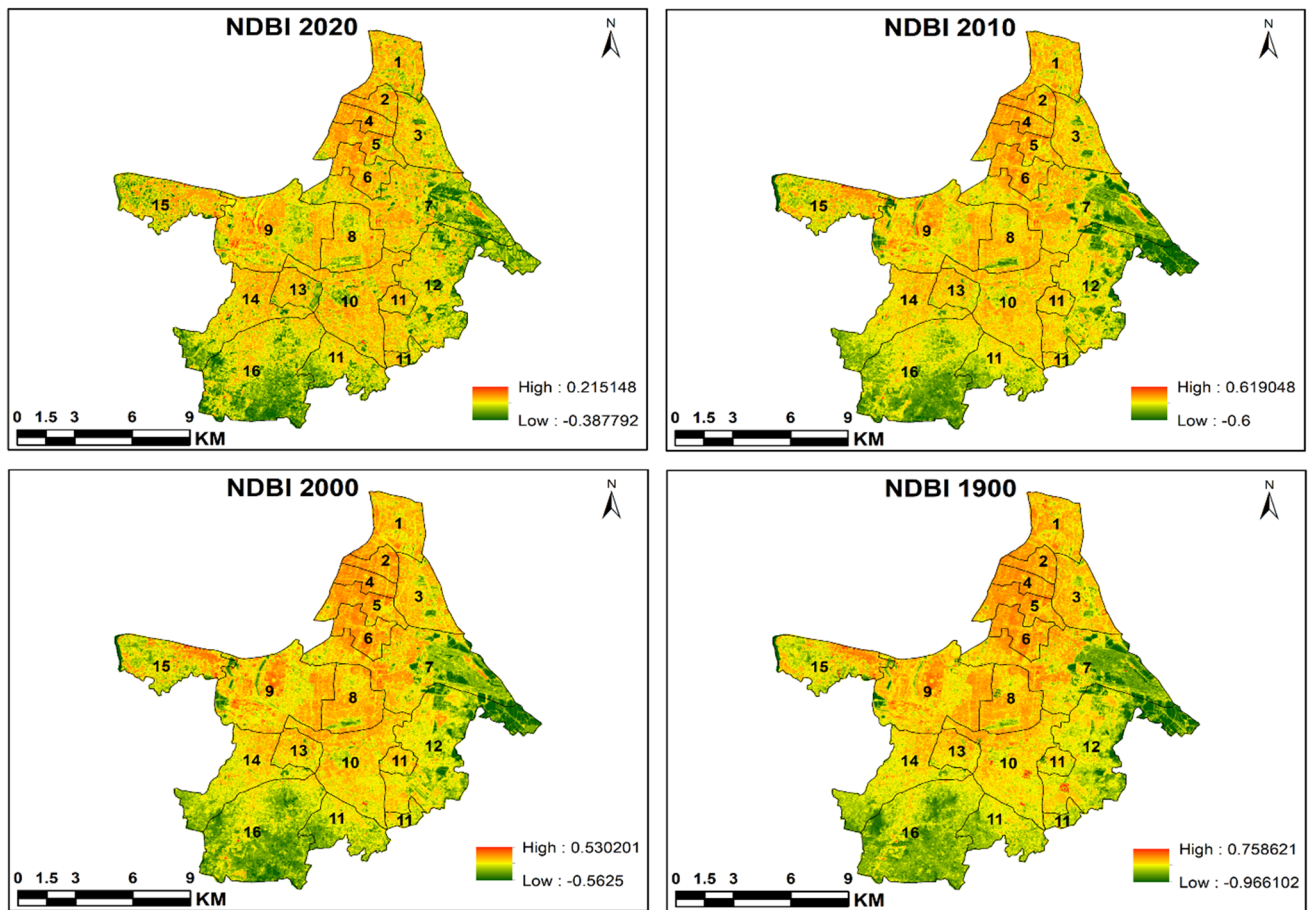


Fig. 5 Maps of decadal and overall transformation in normalized difference vegetation index (1990–2020)

**Table 2** Borough wise recorded highest and lowest NDBI for 2020, 2010, 2000, and 1990

Boroughs	2020		2010		2000		1990	
	Highest	Lowest	Highest	Lowest	Highest	Lowest	Highest	Lowest
1	0.139	-0.311	0.425	-0.290	0.400	-0.250	0.603	-0.634
2	0.124	-0.253	0.372	-0.120	0.347	-0.093	0.371	-0.135
3	0.169	-0.290	0.550	-0.355	0.389	-0.368	0.648	-0.545
4	0.105	-0.222	0.369	-0.200	0.322	-0.125	0.603	-0.386
5	0.168	-0.230	0.619	-0.200	0.333	-0.235	0.617	-0.343
6	0.177	-0.329	0.388	-0.186	0.346	-0.127	0.411	-0.429
7	0.201	-0.380	0.431	-0.600	0.530	-0.429	0.759	-0.963
8	0.157	-0.278	0.387	-0.294	0.408	-0.286	0.708	-0.441
9	0.187	-0.350	0.487	-0.355	0.463	-0.353	0.667	-0.966
10	0.215	-0.321	0.487	-0.231	0.431	-0.231	0.646	-0.625
11	0.132	-0.356	0.400	-0.353	0.350	-0.333	0.571	-0.449
12	0.167	-0.369	0.394	-0.586	0.435	-0.563	0.694	-0.882
13	0.126	-0.327	0.383	-0.235	0.364	-0.280	0.437	-0.385
14	0.141	-0.388	0.397	-0.300	0.351	-0.313	0.375	-0.429
15	0.134	-0.332	0.431	-0.478	0.424	-0.290	0.713	-0.565
16	0.155	-0.357	0.424	-0.422	0.431	-0.389	0.459	-0.596



**Fig. 6** Decadal maps of normalized difference built-up index (1990–2020)

surface temperatures (LST). Moreover, certain scholars contend that the absence of vegetation coverage also contributes to the urban heat island effect (Xiao et al. 2008; Weng et al. 2004). The depicted Fig. 6 portrays the extent and spatial distribution of developed and non-absorbent land in the years 1990, 2000, 2010, and 2020, as indicated by NDBI categories. The expansion and intensity of this land have progressively increased over time due to the growth of the population and urbanization. Figure 14 illustrates the relationship between the normalized difference built-up index and land surface temperature from 1990 to 2020, with the inclusion of a linear regression model in all four instances. The coefficient of determination values for these four decades are 0.4896, 0.542, 0.5455, and 0.4773, all of which strongly indicate that built-up index has a positive impact on surface temperature (Fig. 14).

### 4.3 Spatio-temporal dynamism of thermal condition

Land surface temperature (LST) is a measure of the surface temperature of the earth's land areas. The present tabular

data displays the extreme LST values, both highest and lowest, recorded in various boroughs of the Kolkata Municipal Corporation during the years 1990, 2000, 2010, and 2020 (Fig. 7 and Table 3). Each row signifies a borough, while each column corresponds to a particular year. The column labeled “Highest” indicates the maximum LST recorded in that borough during the specified year, whereas the “Lowest” column displays the minimum LST recorded (Table 3). The LST values are denoted in degrees Celsius. The table offers valuable insights into the spatial and temporal fluctuations in LST across diverse boroughs of the Kolkata Municipal Corporation (Table 3 and Fig. 10). For instance, in borough 1, the highest LST value in 2020 was 31.29 °C, while the lowest was 24.16 °C. This means that in 2020, the area of borough 1 with the highest surface temperature recorded a value of 31.29 °C, while the area with the lowest surface temperature recorded a value of 24.16 °C. The table provided in the subsequent paragraph (Table 3) reveals the existence of fluctuations in average surface temperature values among various boroughs and over a span of time. It is noteworthy that a persistent upward trend in the mean LST can be subject to investigation. The proliferation of concrete

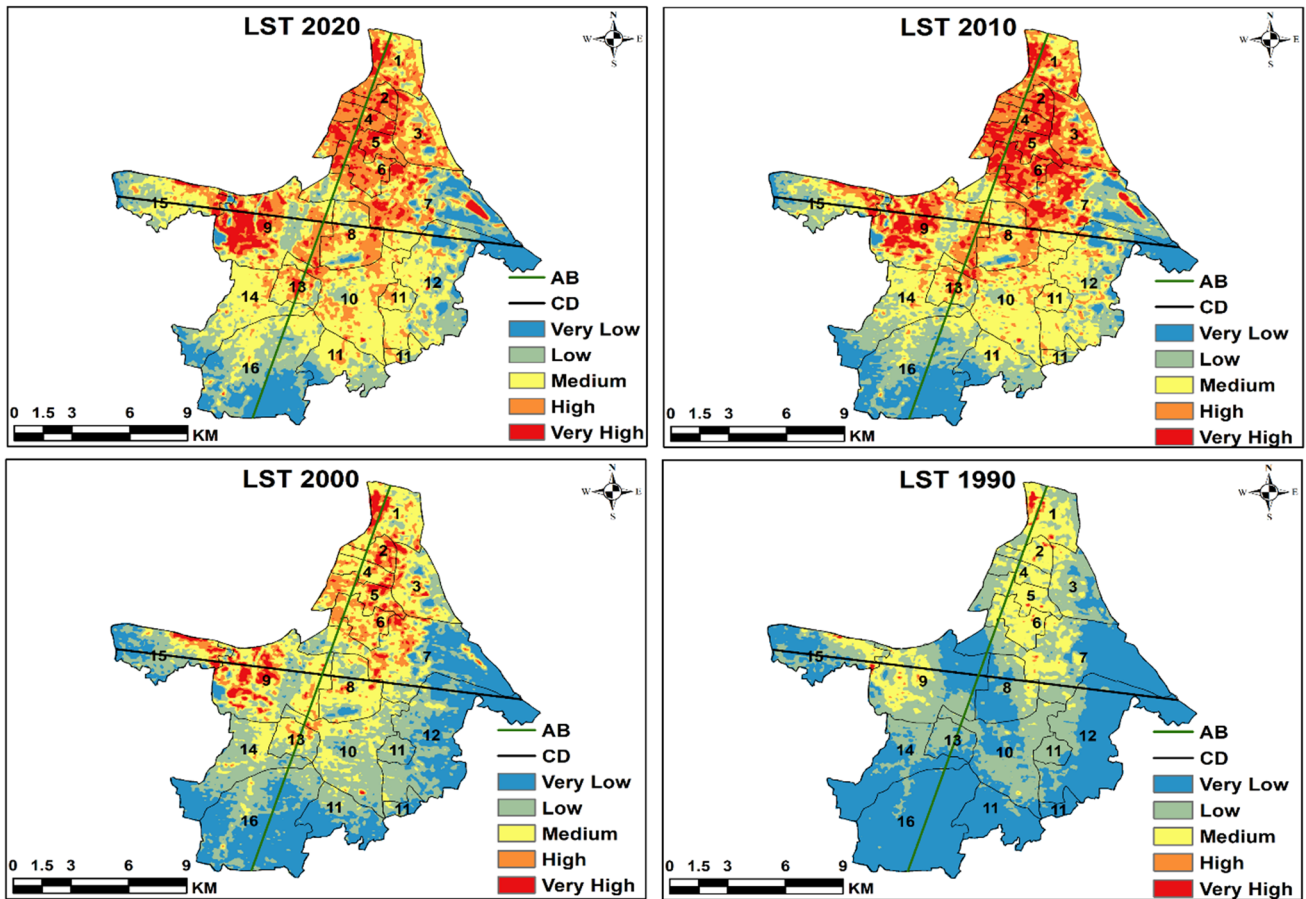


Fig. 7 Decadal maps of surface temperature (1990–2020)

**Table 3** Borough wise recorded highest and lowest LST for 2020, 2010, 2000, and 1990

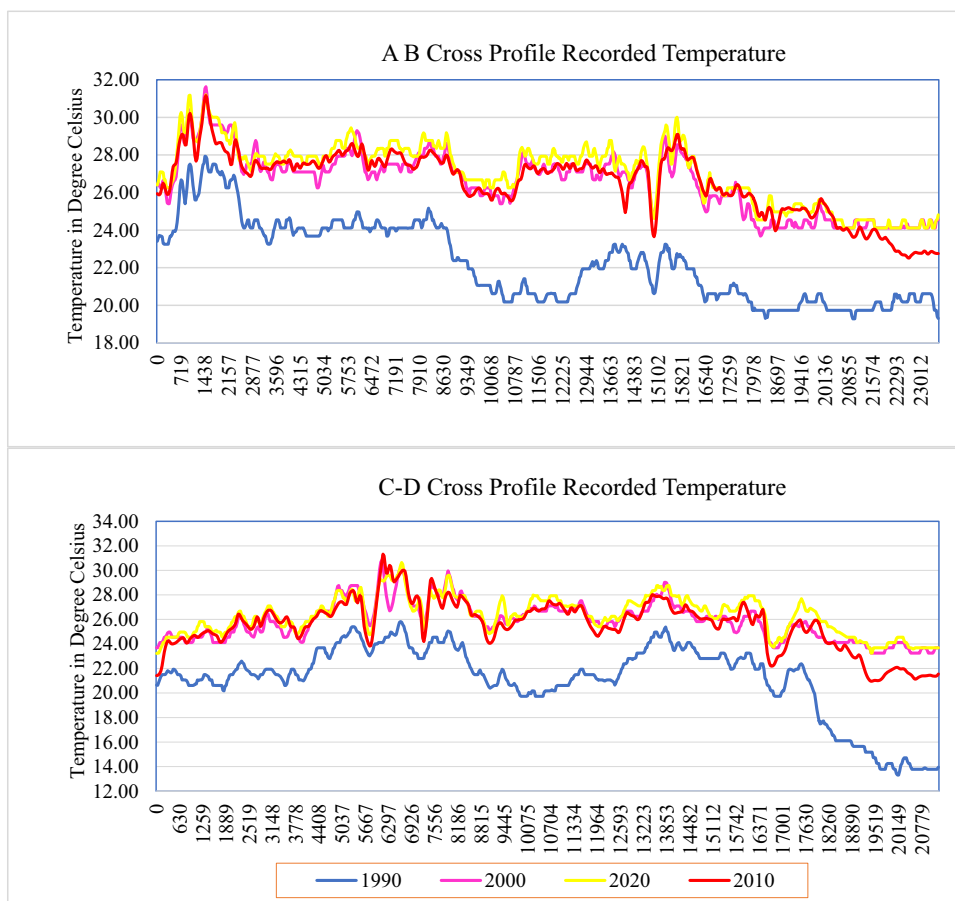
Boroughs	2020		2010		2000		1990	
	Highest	Lowest	Highest	Lowest	Highest	Lowest	Highest	Lowest
1	31.29	24.16	31.65	24.97	32.46	24.55	30.01	21.06
2	30.22	25.48	31.24	26.25	31.24	25.83	25.83	22.82
3	30.80	22.79	31.24	24.11	31.24	23.68	27.93	18.83
4	30.11	25.76	31.24	25.83	30.83	25.83	25.83	22.82
5	30.74	24.00	31.24	25.40	31.65	24.55	27.93	21.06
6	30.22	24.39	30.83	24.55	30.42	24.55	27.52	23.25
7	32.83	21.43	33.70	22.38	31.24	22.82	27.52	13.31
8	30.22	22.77	31.65	24.11	30.01	23.68	27.10	18.83
9	33.00	22.29	32.86	23.25	32.46	23.68	27.93	18.83
10	30.47	24.01	30.83	24.55	31.24	24.11	26.67	18.83
11	27.71	22.44	27.93	23.25	27.10	23.68	23.68	18.83
12	29.79	20.90	29.18	22.40	27.93	22.82	24.55	10.90
13	29.50	23.48	30.01	24.55	29.18	24.97	23.68	20.18
14	28.59	22.66	28.77	23.25	29.60	23.25	23.68	19.73
15	31.74	22.86	32.05	24.11	32.86	23.68	28.35	19.73
16	28.77	22.20	28.77	23.25	28.35	22.38	24.11	17.93

surfaces, industrial production units, transportation systems, and the decline of water bodies and trees in urban areas lead to a surge in anthropogenic heat. This results in the central region of the city becoming hotter than its periphery, producing the urban heat island effect (Fig. 7). In comparison to the surrounding rural landscape, the surface temperature and mean surface temperature increase in urban areas. The increase in developed areas is closely linked to the upsurge in urban heat island trends, which indirectly confirms the

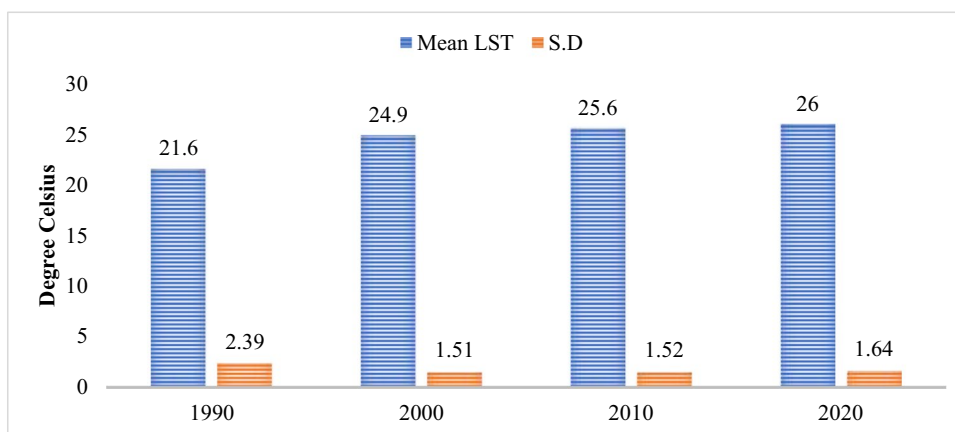
correlation between urbanization and elevated temperatures (Fig. 10).

The major observations that can be made from the table includes that the overall temperature range of the Kolkata Municipal Corporation region falls between 20°C and 35 °C, as indicated by the LST values across all boroughs and years and mean decadal temperatures ranges 21.6°C to 26 °C (Fig. 9). Also, there are yearly variations in surface temperature values between different boroughs as well as same

**Fig. 8** Cross profile recorded temperature for the years 1990, 2000, 2010, and 2020



**Fig. 9** Mean land surface temperature



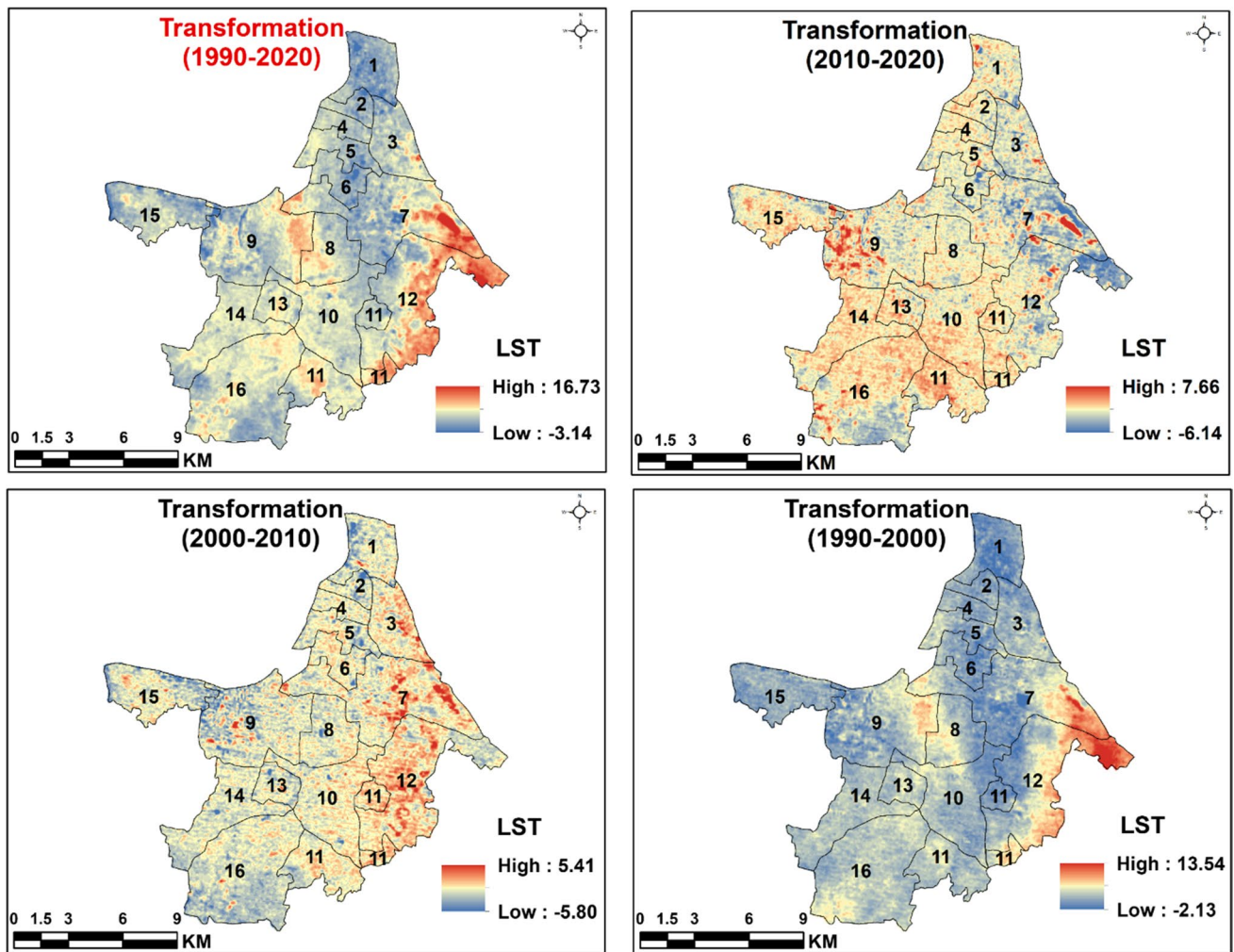


**Fig. 10** Spatio-temporal transformation of surface temperature (1990–2020)

places recorded very fluctuating thermal condition over the last three decades (Fig. 8). For instance, borough 1 experienced an increase in its highest surface temperature value from 30.01 °C in 1990 to 31.29 °C in 2020, while its lowest surface temperature value increased from 21.06 °C in 1990 to 24.16 °C in 2020. The LST values of different boroughs vary, suggesting spatial variations in surface temperatures (Fig. 9). Borough 7 consistently displays higher LST values compared to other boroughs across all years. Possible factors that could influence surface temperature in the study area include the urban heat island effect, land use and land cover changes, climate and weather patterns, and heat mitigation strategies. Boroughs with higher levels of urbanization, characterized by more buildings, concrete surfaces, and less vegetation, tend to have higher surface temperature due to increased absorption and retention of heat. Changes in land use, such as deforestation and urban expansion, can also

impact surface temperature. Climate and weather patterns, including temperature, humidity, wind, and cloud cover, can affect the amount of solar radiation absorbed by the land surface, thereby impacting surface temperature (Fig. 10). Lastly, boroughs that have implemented heat mitigation strategies, such as the creation of green spaces, tree planting, or the use of cool materials in urban infrastructure, may experience lower surface temperature compared to boroughs without such measures. The relationship between the NDVI and LST has been proved by taking the GCP samples as shown in Fig. 12 and regression graphs as well shown in Fig. 13. But based solely on the table, it is difficult to determine clear temporal trends in thermal variations. So, further analysis and comparison with additional data would be required to identify any significant patterns or trends. Also, more additions are necessary to establish the precise reasons behind the observed thermal patterns.

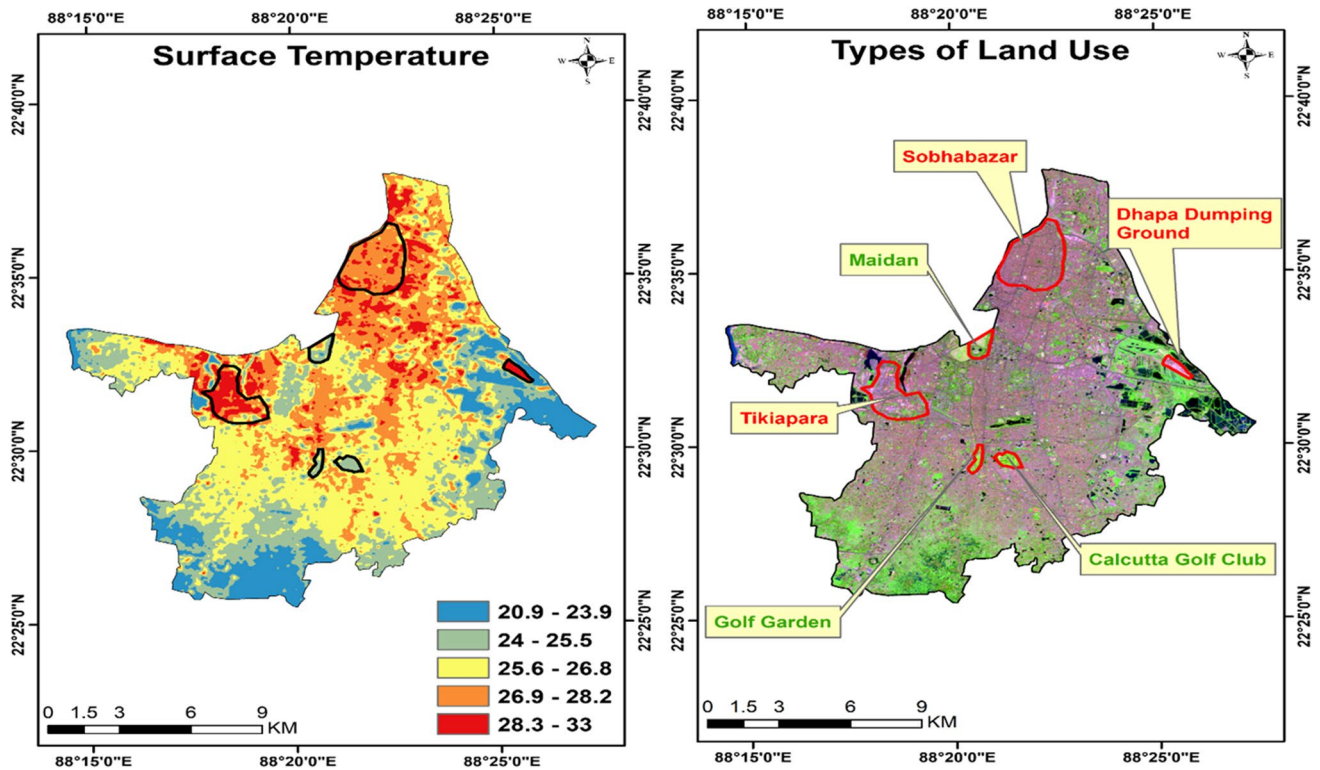


Fig. 11 Types of land use and recorded surface temperature

#### 4.4 Types of land use and their associations with surface temperature

Areas characterized by elevated vegetation index values, such as Maidan, Golf Garden, and Calcutta Golf Club, exhibit a

decline in surface temperatures (Fig. 11). The utilization of vegetation index as a metric for assessing the density and vitality of vegetation is noteworthy. The presence of vegetation offers shade, promotes evaporative cooling, and mitigates surface heat absorption, consequently resulting in reduced temperatures.

**Table 4** Borough wise recorded highest and lowest NDVI, NDBI, and LST for 1990

Boroughs	NDVI		NDBI		LST	
	Highest	Lowest	Highest	Lowest	Highest	Lowest
1	0.655	-0.474	0.603	-0.634	30.01	21.06
2	0.443	-0.476	0.371	-0.135	25.83	22.82
3	0.588	-0.333	0.648	-0.545	27.93	18.83
4	0.519	-0.278	0.603	-0.386	25.83	22.82
5	0.518	-0.561	0.617	-0.343	27.93	21.06
6	0.553	-0.446	0.411	-0.429	27.52	23.25
7	0.705	-0.682	0.759	-0.963	27.52	13.31
8	0.645	-0.690	0.708	-0.441	27.10	18.83
9	0.741	-0.534	0.667	-0.966	27.93	18.83
10	0.652	-0.563	0.646	-0.625	26.67	18.83
11	0.687	-0.436	0.571	-0.449	23.68	18.83
12	0.685	-0.836	0.694	-0.882	24.55	10.90
13	0.667	-0.540	0.437	-0.385	23.68	20.18
14	0.641	-0.632	0.375	-0.429	23.68	19.73
15	0.766	-0.340	0.713	-0.565	28.35	19.73
16	0.695	-0.333	0.459	-0.596	24.11	17.93

**Table 5** Borough wise recorded highest and lowest NDVI, NDBI, and LST for 2000

Boroughs	NDVI		NDBI		LST	
	Highest	Lowest	Highest	Lowest	Highest	Lowest
1	0.417	-0.170	0.400	-0.250	32.46	24.55
2	0.275	-0.094	0.347	-0.093	31.24	25.83
3	0.469	-0.167	0.389	-0.368	31.24	23.68
4	0.259	-0.132	0.322	-0.125	30.83	25.83
5	0.406	-0.191	0.333	-0.235	31.65	24.55
6	0.377	-0.115	0.346	-0.127	30.42	24.55
7	0.496	-0.160	0.530	-0.429	31.24	22.82
8	0.462	-0.137	0.408	-0.286	30.01	23.68
9	0.477	-0.259	0.463	-0.353	32.46	23.68
10	0.478	-0.107	0.431	-0.231	31.24	24.11
11	0.473	-0.098	0.350	-0.333	27.10	23.68
12	0.472	-0.143	0.435	-0.563	27.93	22.82
13	0.504	-0.132	0.364	-0.280	29.18	24.97
14	0.521	-0.102	0.351	-0.313	29.60	23.25
15	0.472	-0.292	0.424	-0.290	32.86	23.68
16	0.548	-0.148	0.431	-0.389	28.35	22.38

Furthermore, the availability of green spaces in these areas facilitates enhanced air circulation and ventilation, thereby aiding in the dissipation of heat and subsequent reduction of surface temperatures. Additionally, these regions demonstrate low built-up index values, indicating a reduced concentration of constructed structures. The decreased density of built-up areas implies lesser degree of heat absorption and retention, thereby contributing to the decrease in surface temperatures.

Areas characterized by intense urban activities, such as Sobhabazar, Tikiapara, and the vicinity of the Dhapa dumping ground, tend to have higher surface temperatures (Fig. 11). This is primarily due to the heat absorption and retention by

buildings and infrastructure in these areas, which leads to an increase in surface temperatures. The presence of built-up density and infrastructure in areas like Sobhabazar, Tikiapara, and near the Dhapa Dumping Ground contributes to the accumulation of heat, resulting in augmented surface temperatures.

#### 4.5 Association among vegetation index, built-up index, and thermal conditions

From Fig. 7 and the graph, it is estimated that there is continuous increase in the surface temperature of the KMC from the years 1990 to 2020. The change could be

**Table 6** Borough wise recorded highest and lowest NDVI, NDBI, and LST for 2010

Boroughs	NDVI		NDBI		LST	
	Highest	Lowest	Highest	Lowest	Highest	Lowest
1	0.527	-0.217	0.425	-0.290	31.65	24.97
2	0.437	-0.086	0.372	-0.120	31.24	26.25
3	0.562	-0.189	0.550	-0.355	31.24	24.11
4	0.419	-0.137	0.369	-0.200	31.24	25.83
5	0.476	-0.200	0.619	-0.200	31.24	25.40
6	0.449	-0.107	0.388	-0.186	30.83	24.55
7	0.613	-0.209	0.431	-0.600	33.70	22.38
8	0.505	-0.179	0.387	-0.294	31.65	24.11
9	0.541	-0.375	0.487	-0.355	32.86	23.25
10	0.556	-0.106	0.487	-0.231	30.83	24.55
11	0.533	-0.156	0.400	-0.353	27.93	23.25
12	0.600	-0.265	0.394	-0.586	29.18	22.40
13	0.575	-0.163	0.383	-0.235	30.01	24.55
14	0.565	-0.163	0.397	-0.300	28.77	23.25
15	0.603	-0.375	0.431	-0.478	32.05	24.11
16	0.583	-0.149	0.424	-0.422	28.77	23.25



**Table 7** Borough wise recorded highest and lowest NDVI, NDBI, and LST for 2020

Boroughs	NDVI		NDBI		LST	
	Highest	Lowest	Highest	Lowest	Highest	Lowest
1	0.467	-0.047	0.139	-0.311	31.29	24.16
2	0.416	0.012	0.124	-0.253	30.22	25.48
3	0.478	-0.057	0.169	-0.290	30.80	22.79
4	0.378	-0.041	0.105	-0.222	30.11	25.76
5	0.405	-0.091	0.168	-0.230	30.74	24.00
6	0.479	-0.014	0.177	-0.329	30.22	24.39
7	0.485	-0.073	0.201	-0.380	32.83	21.43
8	0.423	-0.072	0.157	-0.278	30.22	22.77
9	0.483	-0.094	0.187	-0.350	33.00	22.29
10	0.480	-0.098	0.215	-0.321	30.47	24.01
11	0.473	-0.059	0.132	-0.356	27.71	22.44
12	0.496	-0.159	0.167	-0.369	29.79	20.90
13	0.456	-0.063	0.126	-0.327	29.50	23.48
14	0.556	-0.048	0.141	-0.388	28.59	22.66
15	0.478	-0.088	0.134	-0.332	31.74	22.86
16	0.556	-0.086	0.155	-0.357	28.77	22.20

profoundly found in Fig. 7 and the trend of rising temperature is clearly visible. In 1990, the temperature was high in the left side only in a patch but during 2000 it got increased and covered more wards to the left and right of the patch. It again increased in 2010 inculcating few more wards in it and finally in 2020, it modifies the temperature of large number of wards. The probable reason for this drastic change leads to increase in built-up and reduction in green space and NDVI value of the concerned area (Table 4, 5, 6, 7). The cross profile of recorded

surface temperature (Fig. 8) has highlighted the significant changes in LST with the passage of time during different time periods. The present study has determined that a high land surface temperature is associated with low green cover. Therefore, the cooling effects of green cover can offer valuable guidance for the planning and design of urban climates (Hang and Rahman 2018a, b). It has been found that there is a consistent decrease in green space, an increase in land surface temperature, and a reduction in the overall area of green cover. These negative indicators have

**Fig. 12** GCP sample sites

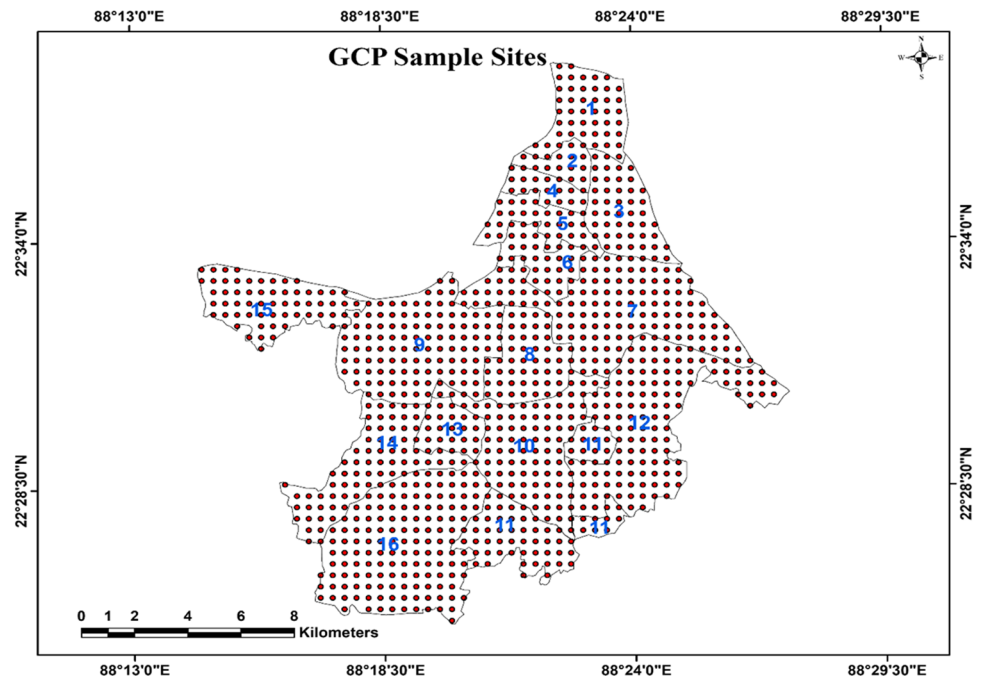
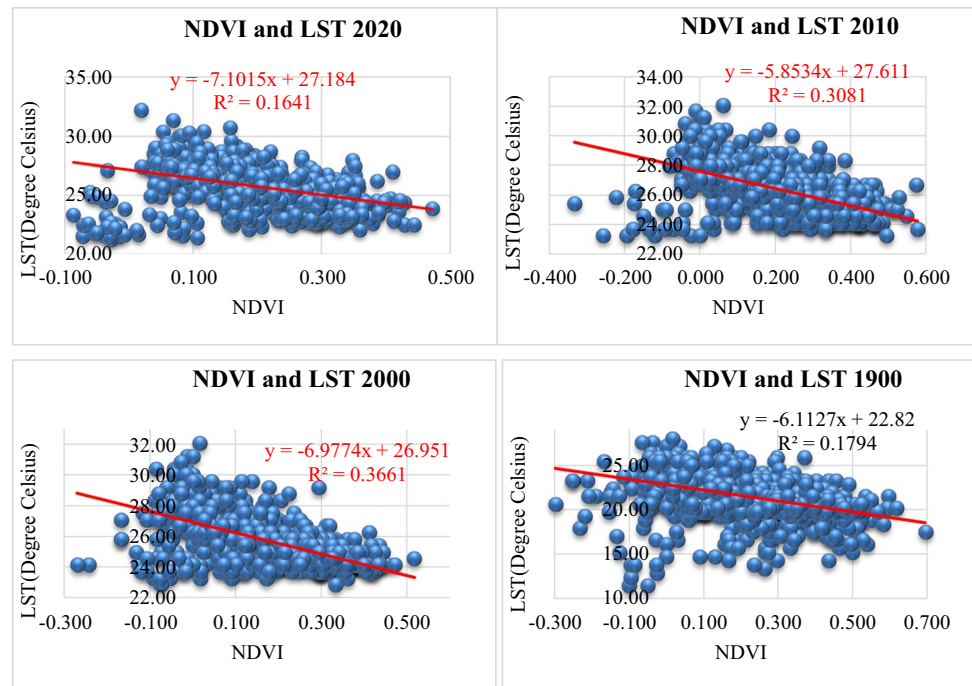


**Fig. 13** Relationship between vegetation index and surface temperature

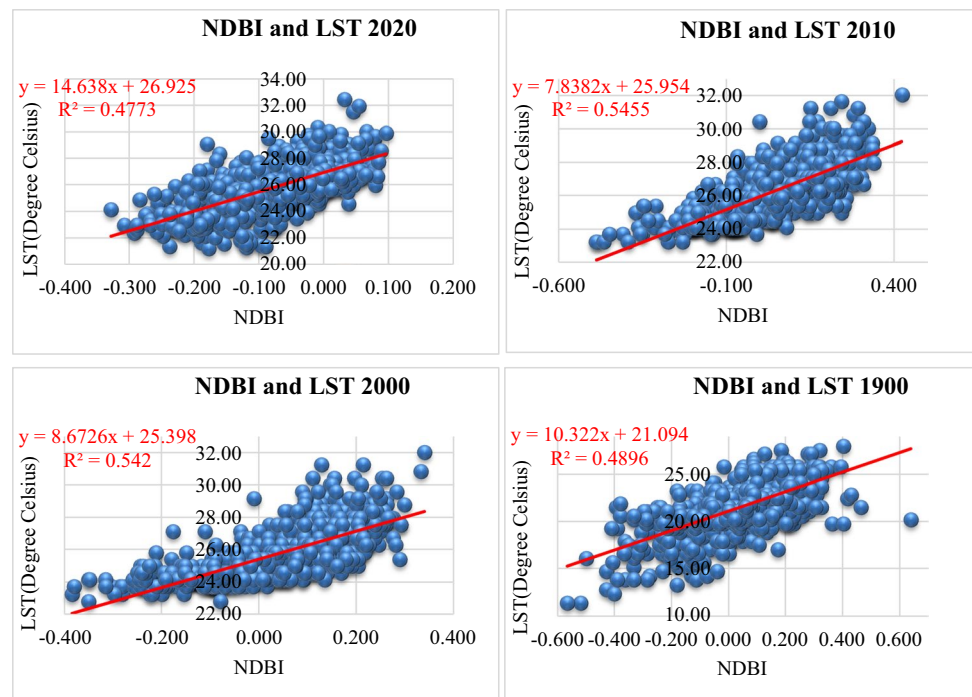


detrimental effects on ecological balance (Rosenberg et al. 1983; Morton 1983; Rai 2016). The reduction of green spaces is mainly attributed to rapid population growth and constructional activities, particularly in tier I cities such as the Kolkata metropolitan region (Sieghardt et al. 2005; Owen et al. 2006). The reason behind this association is

that green cover plays a crucial role in cooling urban climates through various mechanisms.

Green cover provides shade, which helps to reduce the amount of direct sunlight reaching the ground and subsequently lowers surface temperatures. Additionally, plants release moisture through a process called

**Fig. 14** Relationship between built-up index and surface temperature



transpiration, which cools the surrounding air. This evapotranspiration process contributes to the overall cooling effect of green spaces. The cooling effects of green spaces have significant implications for the planning and design of urban areas. By incorporating green spaces, such as parks, gardens, and trees, into urban planning, it is possible to mitigate the heat island effect and create more comfortable living environments. This can be particularly important in densely populated cities where the concentration of buildings and infrastructure can lead to higher temperatures. As cities expand and urbanize, there is often a need for more infrastructure and housing, leading to the conversion of green areas into built-up spaces (Fig. 12).

The present study emphasizes the importance of green spaces in mitigating high land surface temperatures and offers valuable guidance for urban climate planning and design (Figs. 13 and 14). The consistent decrease in green spaces, increase in land surface temperature, and reduction in green cover have negative consequences for ecological balance. These trends are primarily driven by rapid population growth and construction activities in urban areas.

## 5 Conclusion and suggestions

The Kolkata Municipal Corporation (KMC) holds a pivotal role in shaping the city's future, particularly concerning urban green spaces, which are crucial for a livable city, offering ecological, environmental, social, and economic benefits. The study reveals a range of land surface temperatures (LST) within the region, indicating variations across boroughs and years. Some boroughs exhibit increasing surface temperatures over time, while others show a decreasing trend. Spatial disparities in LST values are apparent, with certain boroughs consistently displaying higher temperatures. The observed variations can be attributed to factors like the urban heat island effect, land use changes, climate patterns, and mitigation strategies. Prioritizing the development and maintenance of urban green spaces by KMC can enhance citizens' quality of life, addressing environmental challenges and promoting sustainability. Key benefits include improved air and water quality, reduced heat island effect, enhanced biodiversity, and recreational opportunities, translating into improved public health, increased property values, and economic benefits. Facing challenges like air and water pollution and diminishing green spaces due to rapid urbanization, KMC should focus on sustainable development through green infrastructure, renewable energy, and emissions reduction. Regular monitoring and evaluation, guided by key performance indicators, are essential for ensuring the effectiveness of urban planning initiatives. The study fills a

research gap by analyzing the spatio-temporal transformation of urban green spaces in KMC, employing environmental indices and transformations. While past studies focused on other megacities, this research uniquely examines Kolkata's dynamics, providing valuable insights into its urban environment. The study's significance lies in describing and evaluating the transformation of green spaces and its impact on environmental factors, addressing a critical research gap. The ward-wise analysis enhances understanding, yet future studies could incorporate percentage changes in area for a more comprehensive assessment.

**Acknowledgements** The authors would like to thank Aligarh Muslim University, India, and the Department of Geography of Aligarh Muslim University for supporting and providing with infrastructural facilities for completing this study.

**Author contributions** Author Contributions: Conceptualization: Md Babor Ali and Saleha Jamal Data monitoring: Md Babor Ali Methodology: Md Babor Ali Data curation: Md Babor Ali Mapping: Md Babor Ali Formal analysis: Md Babor Ali, Saleha Jamal, Manal Ahmad and Mohd Saqib Final Review: Md Babor Ali and Saleha Jamal

**Funding** The authors declare that no funds, grants, or other support were received during the preparation of this manuscript. The authors would like to thank UGC for providing SRF fellowship for Ph.D.

**Data availability** All the data generated and analyzed during this study are available on request from the corresponding author.

Data used in this research has not been used earlier elsewhere.

## Declarations

**Ethics approval** Not applicable to this study.

**Consent to participate** Every author has equal participation.

**Consent for publication** This research work is novel and nowhere has been submitted for publication.

**Competing interests** The authors declare no competing interests.

## References

- Ajmal U, Jamal S, Ahmad WS, Ali MA, Ali MB (2022) Waterborne diseases vulnerability analysis using fuzzy analytic hierarchy process: a case study of Azamgarh city India. *Model Earth Syst Environ* 8(2):2687–2713
- Alavipanah S, Wegmann M, Qureshi S, Weng Q, Koellner T (2015) The role of vegetation in mitigating urban land surface temperatures: a case study of Munich Germany during the Warm Season. *Sustainability* 7(4):4689–4706
- Asgarian A, Amiri BJ, Sakieh Y (2015) Assessing the effect of green cover spatial patterns on urban land surface temperature using landscape metrics approach. *Urban Ecosystem* 18(1):209–222. <https://doi.org/10.1007/s11252-014-0387-7>
- Badarinath KVS, Kiran Chand TR, Madhavilatha K, Raghavaswamy V (2005) Studies on urban heat islands using envisat AATSR data. *J Indian Soc Remote Sens* 33(4):495–501

- Becker F, Li Z-L (1990) Toward a local split-window method over land surface. *Int J Remote Sens* 11(3):369–393. <https://doi.org/10.1080/01431169008955028>
- Bindi M, Brandani G, Dessì A, Dibari C, Ferrise R, Moriondo M, Trombi G (2009) Impact of climate change on agricultural and natural ecosystems. *Am J Environ Sci* 5(5):633–638
- Buyadi S, Mohd W, Misni A (2013) Impact of land use changes on the surface temperature distribution of area surrounding the National Botanic Garden, Shah Alam. *Procedia Soc Behav Sci* 101:516–525
- Carrus G, Scopelliti M, Laforteza R, Colangelo G et al (2015) Go greener, feel better? The positive effects of biodiversity on the well-being of individuals visiting urban and peri-urban green areas. *Landsc Urban Plan* 134:221–228. <https://doi.org/10.1016/j.landurbplan.2014.10.022>
- Chadchan J, Shankar R (2012) An analysis of urban growth trends in the post-economic reforms period in India. *Int J Sustain Built Environ* 1(1):36–49
- Chen YH, Wang J, Li XB (2002) A study on urban thermal field in summer based on satellite remote sensing. *Remote Sens Land Resour* 4(1)
- Chen XL, Zhao HM, Li PX, Yin ZY (2006) Remote sensing image-based analysis of the relationship between urban heat island and land use/cover changes. *Remote Sens Environ* 104(2):133–146
- Chudnovsky A, Ben-Dor E, Saaroni H (2004) Diurnal thermal behavior of selected urban objects using remote sensing measurements. *Energy Build* 36:1063–1074. <https://doi.org/10.1016/j.enbuild.2004.01.052>
- Demographia world urban areas 13th annual edition. (2017). doi: <https://demographia.com/dbworldua-index.htm>
- Deng C, Wu C (2012) BCI: a biophysical composition index for remote sensing of urban environments. *Remote Sens Environ* 127:247–259. <https://doi.org/10.1016/j.rse.2012.09.009>
- Escobedo FJ, Kroeger T, Wagner JE (2011) Urban forests and pollution mitigation: analyzing ecosystem services and disservices. *Environ Pollut* 159(8–9):2078–2087. <https://doi.org/10.1016/j.envpol.2011.01.010>
- Feng H, Liu H, Wu L (2014) Monitoring the relationship between the land surface temperature change and urban growth in Beijing China. *IEEE J Sel Top Appl Earth Obs Remote Sens* 7(10):4010–4019
- Gairola S, Noresah MS (2010) Emerging trend of urban green space research and the implications for safeguarding biodiversity: a viewpoint. *Nat Sci* 8(7):43–49
- Gao B-C (1996) NDWI—a normalized difference water index for remote sensing of vegetation liquid water from space. *Remote Sens Environ* 58(3):257–266
- García DH, Riza M, Díaz JA (2023) Land surface temperature relationship with the land use/land cover indices leading to thermal field variation in the Turkish Republic of Northern Cyprus. *Earth Syst Environ* 7(2):561–580
- Guo G, Wu Z, Xiao R, Chen Y (2015) Landscape and urban planning impacts of urban biophysical composition on land surface temperature in urban heat island clusters. *Landsc Urban Plan* 135:1–10. <https://doi.org/10.1016/j.landurbplan.2014.11.007>
- Hang HT, Rahman A (2018) Characterization of thermal environment over heterogeneous surface of National Capital Region (NCR), India using LANDSAT-8 sensor for regional planning studies *Urban Climate*:1–18 <https://doi.org/10.1016/j.uclim.2018.01.001>
- Hang HT, Rahman A (2018b) Characterization of thermal environment over heterogeneous surface of National Capital Region (NCR), India using LANDSAT-8 sensor for regional planning studies. *Urban Climate* 24:1–18. <https://doi.org/10.1016/j.uclim.2018.01.001>
- Hao P, Niu Z, Zhan Y, Wu Y, Wang L, Liu Y (2016) Spatiotemporal changes of urban impervious surface area and land surface temperature in Beijing from 1990 to 2014. *Gisci Remote Sens* 53(1):63–84. <https://doi.org/10.1080/15481603.2015.1095471>
- Hartmann DL, Tank AM GK, & Rusticucci M (2013) IPCC 5th assessment report, climate change 2013: the physical science basis. In Paper presented at the IPCC
- S Jamal MB Ali 2023 Determining urban growth in response to land use dynamics using multilayer perceptron and Markov chain models in a metropolitan city: past and future *Environ Dev Sustain* 1 27
- Jamal S, Ahmad WS, Ajmal U, Aaquib M, Ashif Ali M, Babor Ali M, Ahmed S (2022a) An integrated approach for determining the anthropogenic stress responsible for degradation of a Ramsar Site-Wular Lake in Kashmir India. *Mar Geodesy* 45(4):407–434
- Jamal S, Ali MB, Ali MA, Ajmal U (2022b) Evaluation and distribution of urban green spaces in Kolkata Municipal Corporation: an approach to urban sustainability. Towards sustainable natural resources: monitoring and managing ecosystem biodiversity. Springer International Publishing, Cham, pp 151–172
- Jamal S, Saqib M, Ahmad WS, Ahmad M, Ali MA, Ali MB (2023) Unraveling the complexities of land transformation and its impact on urban sustainability through land surface temperature analysis. *Appl Geomatics* 15(3):719–41
- Jim CY, Chen WY (2008) Assessing the ecosystem service of air pollutant removal by urban trees in Guangzhou (China). *J Environ Manage* 88(4):665–676
- Karuppanan S, Baharuddin ZM, Sivam A, Daniels CB (2014) Urban green space and urban biodiversity: Kuala Lumpur Malaysia. *J Sustain Dev* 7(1). <https://doi.org/10.5539/jsd.v7n1p1>
- Kaufmann RK, Zhou L, Myneni RB, Tucker CJ, Slayback D, Shabanov NV, Pinzon J (2003) The effect of vegetation on surface temperature: a statistical analysis of NDVI and climate data. *Geophys Res Lett* 30 (22)
- Konijnendijk CC, Annerstedt M, Nielsen AB & Maruthaveeran S (2013) Benefits of urban parks. A systematic review A Report for IFPRA, Copenhagen & Alnarp. <https://www.forskningdatabasen.dk/en/catalog/2389131353>
- Kumar KS, Bhaskar PU, Padma Kumari K (2012) Estimation of land surface temperature to study urban heat island effect using Landsat ETM + IMAGE. *Int J Eng Sci Technol* 4(02):771–778
- Li CH, Yang ZF (2004) Spatio-temporal changes of NDVI and their relations with precipitation and Run of in the Yellow River Basin. *Geogr Res* 23:753–759
- Li X, Chen G, Liu X, Liang X, Wang S, Chen Y, Xu X (2017) A new global land-use and land-cover change product at a 1-km resolution for 2010 to 2100 based on human–environment interactions. *Ann Am Assoc Geogr* 107(5):1040–1059
- Lillesand T, Kiefer RW, Chipman J (2015) Remote sensing and image interpretation. John Wiley & Sons
- Loehle C, Scafetta N (2011) Climate change attribution using empirical decomposition of climatic data. *Open Atmos Sci J* 5:1–4. <https://doi.org/10.2174/1874282301105010074>
- Ma Y, Kuang Y, Huang N (2010) Coupling urbanization analyzes for studying urban thermal environment and its interplay with biophysical parameters based on TM/ETM+imagery. *Int J Appl Earth Obs Geoinf* 12(2):110–118. <https://doi.org/10.1016/j.jag.2009.12.002>
- Mallick J, Kant Y, Bharath BD (2008) Estimation of land surface temperature over Delhi using Landsat-7 ETM. *J Ind Geophys Union* 12(3):131–140
- Mallick J, Rahman A, Singh CK (2013) Modeling urban heat islands in heterogeneous land surface and its correlation with impervious surface area by using nighttime ASTER satellite data in highly urbanizing city, Delhi-India. *Adv Space Res* 52:639–655. <https://doi.org/10.1016/j.asr.2013.04.025>

- Mass JF (1999) Monitoring land-cover changes: a comparison of change detection techniques. *Int J Remote Sens* 20(1):139–152
- Mathew A, Sree Kumar S, Khandelwal S, Kaul N, Kumar R (2016) Prediction of surface temperatures for the assessment of urban heat island effect over Ahmedabad city using linear time series model. *Energy Build* 128:605–616. <https://doi.org/10.1016/j.enbuild.2016.07.004>
- McKinney ML (2002) Urbanization, biodiversity, and conservation. *Bioscience* 52:883–890
- Moghadam HS, Helbich M (2013) Spatiotemporal urbanization processes in the megacity of Mumbai, India: a Markov chains-cellular automata urban growth model. *Appl Geogr* 40:140–149. <https://doi.org/10.1016/j.apgeog.2013.01.009>
- Mohammad P, Goswami A (2022) Predicting the impacts of urban development on seasonal urban thermal environment in Guwahati city, northeast India. *Build Environ* 226:109724
- Mohan M, Kandya A (2015) Impact of urbanization and land-use/land-cover change on diurnal temperature range: a case study of tropical urban airshed of India using remote sensing data. *Sci Total Environ* 506:453–465. <https://doi.org/10.1016/j.scitotenv.2014.11.006>
- Morton FI (1983) Operational estimates of areal evapotranspiration and their significance to the science and practice of hydrology. *J Hydrol* 66(1–4):1–76. [https://doi.org/10.1016/0022-1694\(83\)90177-4](https://doi.org/10.1016/0022-1694(83)90177-4)
- Mushore T, Mutanga O, Odindi J, Dube T (2017) Linking major shifts in land surface temperatures to long term land use and land cover changes: a case of Harare, Zimbabwe. *Urban Climate* 20:120–134. <https://doi.org/10.1016/j.uclim.2017.04.005>
- Naikoo MW, Islam ARMT, Mallick J, Rahman A (2022) Land use/land cover change and its impact on surface urban heat island and urban thermal comfort in a metropolitan city. *Urban Climate* 41:101052
- Nayak S, & Mandal M (2012) Impact of land-use and land-cover changes on temperature trends over western India. *Current Science*, 102 <https://www.jstor.org/stable/24107759>
- Nowak DJ, Robert III E, Crane DE, Stevens JC, & Fisher CL (2010) Assessing urban forest effects and values, Chicago's urban forest Resour Bull NRS-37 (pp. 1–27). Newtown Square, PA: US Department of Agriculture, Forest Service, Northern Research Station 27
- Oliveira S, Andrade H, Vaz T (2011) The cooling effect of green spaces as a contribution to the mitigation of urban heat: a case study in Lisbon. *Build Environ* 46(11):2186–2194. <https://doi.org/10.1016/j.buildenv.2011.04.034>
- Oliveira S, Andrade H, Vaz T (2011b) The cooling effect of green spaces as a contribution to the mitigation of urban heat: a case study in Lisbon. *Build Environ* 46(11):2186–2194
- Owen LA, Pickering KT, Pickering KT (2006) An introduction to global environmental issues. Routledge
- Pandey B, Seto KC (2015) Urbanization and agricultural land loss in India: comparing satellite estimates with census data. *J Environ Manag* 148:53–66
- Pauleit S, Ennos R, Golding Y (2005) Modeling the environmental impacts of urban land use and land cover change—a study in Merseyside UK. *Landscape Urban Plan* 71(2–4):295–310
- Rai PK (2016) Impacts of particulate matter pollution on plants: implications for environmental biomonitoring. *Ecotoxicol Environ Saf* 129:120–136. <https://doi.org/10.1016/j.ecoenv.2016.03.012>
- Rinner C, Hussain M (2011) Toronto's urban heat island—exploring the relationship between land use and surface temperature. *Remote Sens* 3(6):1251–1265. <https://doi.org/10.3390/rs3061251>
- Rosenberg NJ, Blad BL, Verma SB (1983) Microclimate: the biological environment. Wiley, Hoboken
- Rosenzweig C, Solecki W, & Slosberg R (2006) Mitigating New York City's heat island with urban forestry, living roofs, and light surfaces. A report to the New York State Energy Research and Development Authority
- Rotem-Mindali O, Michael Y, Helman D, Lensky IM (2015) The role of local land-use on the urban heat island effect of Tel Aviv as assessed from satellite remote sensing. *Appl Geogr* 56:145–153. <https://doi.org/10.1016/j.apgeog.2014.11.023>
- Salman MA (2004) A modelling approach to cumulative effects assessment for rehabilitation of remnant vegetation. PhD Thesis. SRES, The Australian National University, Canberra, Australia
- Sannigrahi S, Bhatt S, Rahmat S, Uniyal B, Banerjee S, Chakraborti S et al (2018) Analyzing the role of biophysical compositions in minimizing urban land surface temperature and urban heating. *Urban Climate* 24:803–819. <https://doi.org/10.1016/j.uclim.2017.10.002>
- Sarif MO, Gupta RD, Murayama Y (2022) Assessing local climate change by spatiotemporal seasonal LST and six land indices, and their interrelationships with SUHI and hot-spot dynamics: a case study of Prayagraj City, India (1987–2018). *Remote Sens* 15(1):179
- Sertel E, Ormeci C, Robock A (2011) Modelling land cover change impact on the summer climate of the Marmara region Turkey. *Int J Glob Warm* 3(1/2):194
- Shahfahad Bindajam AA, Naikoo MW, Horo JP, Mallick J, Rihan M, ... & Rahman A (2023) Response of soil moisture and vegetation conditions in seasonal variation of land surface temperature and surface urban heat island intensity in sub-tropical semi-arid cities. *Theoretical and Applied Climatology*, 1–29
- Shahfahad Talukdar S, Rihan M, Hang HT, Bhaskaran S & Rahman A (2021) Modelling urban heat island (UHI) and thermal field variation and their relationship with land use indices over Delhi and Mumbai metro cities *Environment, Development and Sustainability* 1–29
- Sieghardt M, Mursch-Radgruber E, Paoletti E, Couenberg E, Dimitrakopoulos A, Rego F et al (2005) The abiotic urban environment: impact of urban growing conditions on urban vegetation. In: Konijnendijk C, Nilsson K, Randrup T, Schipperijn J (eds) *Urban forests and trees*. Springer, Berlin, pp 281–323
- Su S, Xiao R, Jiang Z, Zhang Y (2012) Characterizing landscape pattern and ecosystem service value changes for urbanization impacts at an eco-regional scale. *Appl Geogr* 34:295–305
- The World Resources Institute (1996) *The urban environment: world resources 1996–97*. Oxford University Press, New York
- United Nations (2012) *World urbanization prospects: the 2011 revision*. United Nations, New York
- United Nations Department of Economic and Social Affairs (UNDESA) (2012) *Nations Department of Economic and Social Affairs. World urbanization prospects: the 2011 revision*. New York: United Nations Department of Economic and Social Affairs/Population Division
- Ward DS, Mahowald NM, Kloster S (2014) Potential climate forcing of land use and land cover change. *Atmos Chem Phys* 14(23):12701–12724
- Weng Q (2001) A remote sensing-GIS evaluation of urban expansion and its impact on surface temperature in Zhujiang Delta China. *Int J Remote Sens* 22(10):1999–2014
- Weng Q, Lu D, Schubring J (2004) Estimation of land surface temperature-vegetation abundance relationship for urban heat island studies. *Remote Sens Environ* 89(4):467–483
- Wolch JR, Byrne J, Newell JP (2014a) Urban green space, public health, and environmental justice: the challenge of making cities 'just green enough.' *Landscape Urban Plan* 125:234–244. <https://doi.org/10.1016/j.landurbplan.2014.01.017>

- Wu Z, Chen R, Meadows ME, Sengupta D, Xu D (2019) Changing urban green spaces in Shanghai: trends, drivers and policy implications. *Land Use Policy* 87:104080
- Wu J, Yang M, Xiong L, Wang C, Ta N (2021) Health-oriented vegetation community design: innovation in urban green space to support respiratory health. *Landsc Urban Plan* 205:103973
- Xian G, Crane M, Steinward D (2005) Dynamic modeling of Tampa Bay urban development using parallel computing. *Comput Geosci* 31(7):920–928. <https://doi.org/10.1016/j.cageo.2005.03.006>
- Xiao R, Weng Q, Ouyang Z, Li W, Schienke EW, Zhang Z (2008) Land surface temperature variation and major factors in Beijing China. *Photogramm Eng Remote Sens* 74(4):451–461. <https://doi.org/10.14358/PERS.74.4.451>
- Xu LY, Xie XD, Li S (2013) Correlation analysis of the urban heat island effect and the spatial and temporal distribution of atmospheric particulates using TM images in Beijing. *Environ Pollut* 178:102–114. <https://doi.org/10.1016/j.envpol.2013.03.006>
- Yogesh K, Bharath BD, Mallick J, Atzberger C, Kerle N (2009) Satellite-based analysis of the role of land use: land cover and vegetation density on surface temperature regime of Delhi, India. *J Ind Soc Remote Sens* 37(2):201–214. <https://doi.org/10.1007/s12524-009-0030-x>
- You G, Zhang Y, Liu Y, Schaefer D, Gong H, Gao J, Lu Z, Song Q, Zhao J, Wu C, Yu L, Xie Y (2013) Investigation of temperature and aridity at different elevations of Mt. Ailao SW China. *Int J Biometeorol* 57(3):487–492
- Yuan F, Bauer ME (2007) Comparison of impervious surface area and normalized difference vegetation index as indicators of surface urban heat island effects in Landsat imagery. *Remote Sens Environ* 106(3):375–386
- Yuan F, Sawaya KE, Leofelholz CB, Bauer ME (2005) Land cover classification and change analysis of the twin cities (Minnesota) metropolitan area by multi-temporal Landsat remote sensing. *Remote Sens Environ* 98:317–328. <https://doi.org/10.1016/j.rse.2005.08.006>
- Zha Y, Gao J, Ni S (2003) Use of normalized difference built-up index in automatically mapping urban areas from TM imagery. *Int J Remote Sens* 24(3):583–594
- Zhang B, Xie GD, Gao JX, Yang Y (2014) The cooling effect of urban green spaces as a contribution to energy-saving and emission-reduction: a case study in Beijing China. *Build Environ*. <https://doi.org/10.1016/j.buildenv.2014.03.00>
- Zhang F, Xu N, Wang C, Wu F, Chu X (2020) Effects of land use and land cover change on carbon sequestration and adaptive management in Shanghai, China. *Phys Chem Earth, Parts a/b/c* 120:102948
- Zhou X, Wang YC (2011) Spatial-temporal dynamics of urban green space in response to rapid urbanization and greening policies. *Landsc Urban Plan* 100(3):268–277

**Publisher's Note** Springer Nature remains neutral with regard to jurisdictional claims in published maps and institutional affiliations.

Springer Nature or its licensor (e.g. a society or other partner) holds exclusive rights to this article under a publishing agreement with the author(s) or other rightsholder(s); author self-archiving of the accepted manuscript version of this article is solely governed by the terms of such publishing agreement and applicable law.